PREPARATION AND CHARACTERIZATION OF THERMO AND MAGNETIC RESPONSIVE HYDROGEL PARTICLES FOR REMOVAL OF HEAVY METAL IONS

A thesis submitted in partial fulfillment of the requirement for
the degree of M. Phil. in Chemistry

SUBMITTED BY
FAHIMA TAJRIN
STUDENT ID: 0417033207 F
SESSION: April 2017

Soft and Smart Materials Laboratory
Department of Chemistry
Bangladesh University of Engineering and Technology (BUET)

February, 2021

BANGLADESH UNIVERSITY OF ENGINEERING AND TECHNOLOGY, DHAKA
DEPARTMENT OF CHEMISTRY

PREPARATION AND CHARACTERIZATION OF THERMO AND MAGNETIC RESPONSIVE HYDROGEL PARTICLES FOR REMOVAL OF HEAVY METAL IONS

BY

FAHIMA TAJRIN

has been accepted as satisfactory in partial fulfillment of the requirement for the degree of Master of Philosophy (M.Phil.) in Chemistry and certify that the student has demonstrated a satisfactory knowledge of the field covered by this thesis in an oral examination held on 16th February, 2021.

BOARD OF EXAMINERS

1. Dr. Abu Bin Imran Associate Professor Department of Chemistry BUET, Dhaka (Supervisor)	Chairman
2. Head Department of Chemistry BUET, Dhaka	16/02/21 Member (Ex-Officio)
3. Dr. Md. Shakhawat Hossain Firoz Professor Department of Chemistry BUET, Dhaka	16/02/21 Member
4. Dr. Chanchal Kumar Roy Assistant Professor Department of Chemistry BUET, Dhaka	Member
5. Dr. Md. Aminul Haque Associate Professor Department of Chemistry Jagannath University, Dhaka	Member (External)

CANDIDATE’S DECLARATION

It is hereby declared that this thesis or any part of it has not been submitted elsewhere to award any degree or diploma.

……………………….

Fahima Tajrin

Dedicated to
My Beloved Family

Table of Contents

List of Tables and Figures

List of Figures

List of Table

List of Abbreviations of Terms

1. *N*-isopropylacrylamide(NIPAm)
2. 2-Acrylamido-2-methylpropane sulfonic acid (AMPS)
3. *N*,*N*-methylenebisacrylamide (BIS)
4. Potassium persulfate (KPS)
5. N,N,N′,N′-Tetramethylethane-1,2-diamine (TEMED)
6. Sodium dodecyl sulfate (SDS)
7. Polydopamine (PD)
8. 1,5-diphenylcarbazide (DPC)

Acknowledgment

In the beginning, I humbly acknowledge my deepest gratitude to the almighty, the most gracious, benevolent, and merciful for his infinite mercy bestowed on me in carrying out the research work presented in the dissertation.

It is a great pleasure for me to acknowledge my deepest sense of gratitude, sincere appreciation, heartfelt indebtedness, and solemn regards to my reverend teacher and supervisor, Dr. Abu Bin Imran, Associate Professor, Department of Chemistry, Bangladesh University of Engineering and Technology (BUET), for his kind supervision, indispensable guidance, valuable and constructive suggestions, liberal help and continuous encouragement during the whole period. It is obvious that his attributive contribution and efforts have greatly shaped me into what I am today. I am quite lucky to be a part of his ambitious research team.

It is my great honor to convey my sincere gratitude to my respected teacher Professor Dr. Md. Shakhawat Hossain Firoz, honorable Head of the Department of Chemistry, BUET for giving me his wonderful support to move through the academic processes during this M.Phil. program. I would like to convey my deepest gratitude to Dr. Md. Shafiul Azam, and Dr. Chanchal Kumar Roy of the Department of Chemistry, BUET, for their valuable suggestions, appreciated comments, guidance, and help during the research period.

I am thankful to all other respected teachers of the Department of Chemistry, BUET, for their continuous support. I would also like to thank all of the officers and staff of the Department of Chemistry, BUET, for their relentless help during my study period. I am highly thankful to Dr. Md. Abu Bin Hasan Susan, Professor, Department of Chemistry, University of Dhaka, for helping me during DLS characterizations of my samples.

I am also thankful to my dear consociates and all the members of Soft and Smart Materials Research Group for their friendly cooperation and lovely encouragement throughout my research period. My special thanks to Noman Chowdhury, Sarmin Akter, Solaiman, Tarun Kanti Majumdar, Md. Rezaul Karim, H. B. Muhammad Zukaul Islam, Aminur Rahman, Md. Ferdous and my junior Shayla Chowdhury, for their continuous help during the research

Finally, I would like to express my heartfelt indebtedness and profound gratitude to my beloved father, mother, siblings and my husband for their continuous inspiration and immeasurable sacrifices throughout my study.

Fahima Tajrin

Abstract

The three-dimensional hydrophilic polymeric network of hydrogel achieved unprecedented and unique physicochemical properties with great potential in many fields. Due to the limitations of standard bulk hydrogel submicrometer-sized hydrogel has earned much interest in recent years. The submicrometer-sized hydrogel adds a new dimension to hydrogel research due to its quick stimuli response. Imparting magnetic field into the submicrometer-sized hydrogel provides a new strategy with a variety of additional advantages. The magnetic responsiveness of hydrogels can lead to the generation of functionality under magnetic fields. This work has established a facile route to prepare a dynamic thermo and magnetic responsive submicrometer-sized hydrogel using *N*-Isopropylacrylamide (NIPAM) as monomer and 2-Acrylamido-2-methylpropane sulfonic acid (AMPS) as co-monomer to remove heavy metals from an aquatic environment. Fabrication of magnetic submicrometer-sized hydrogels and their heavy metals removal capacity via electrostatic interactions have been studied systematically. The prepared nanocomposite and submicrometer-sized hydrogels were characterized by Fourier transform infrared (FTIR) spectroscopy, Scanning Electron Microscopy (SEM), Energy dispersive X-ray (EDX) and Dynamic light scattering (DLS). Removal of heavy metal ions from solution by submicrometer-sized hydrogels has been investigated by ultraviolet (UV) spectroscopy. Rare-earth Neodymium magnet is used for the external magnetic field generation. The vast surface area of submicrometer-sized hydrogel particles demonstrates high heavy metal removal effectiveness. Hg^{2+} and $Cr6^{+}$ ions were removed using submicrometer-sized hydrogel particles and removal efficiency is around 167 mg/g and 8 mg/g respectively. The fabricated functional hydrogel particles are strongly magnetic responsive, and heavy metal removal efficiency is good.

CHAPTER 1: Introduction

CHAPTER 2: Experimental

CHAPTER 3: Result & Discussions

CHAPTER 1
Introduction

1. General Introduction

Heavy metals are well-known environmental pollutants due to their toxicity, environmental persistence, and bio-accumulative nature. Their natural sources include weathering of metal-bearing rocks and volcanic eruptions, while anthropogenic sources include mining and various industrial and agricultural activities. Mining and industrial processing for extraction of mineral resources and their subsequent applications for industrial, agricultural, and economic development has led to an increase in the mobilization of these elements in the environment and disturbance of their biogeochemical cycles. Contamination of aquatic and terrestrial ecosystems with toxic heavy metals is a serious environmental problem of public health concerns [1]. Various heavy metals include iron (Fe), zinc (Zn), copper (Cu), manganese (Mn), cobalt (Co), mercury (Hg), arsenic (As), chromium (Cr), lead (Pb), and molybdenum (Mo) with prescribed limit is vital for the human body while above the limit has adverse effects on health and environment [2-3]. Heavy metal toxicity has several consequences on the human body. It can affect the central nervous function leading to mental disorders, damage the blood constituents, and damage the lungs, liver, kidneys, and other vital organs, promoting several disease conditions. The adverse effects of heavy metals in human bodies are vomiting, dehydration, increased blood pressure, kidney damage, bronchitis, gastrointestinal disorder, brain damage, cancer, etc [4]. Hg contamination is very harmful to the human body. It can cause lung damage, gingivitis, spontaneous abortion, protoplasm poisoning. Chronic poisoning of Hg can cause tremors, changes in personality, restlessness, anxiety, sleep disturbance and depression, and so on. High doses may cause death [5]. The specific sources of chromium are leather tanning, electroplating, nuclear power plants, and textile industries. Chromium(VI) is an oxidizing agent, carcinogenic in nature, and harmful to plants and animals [6]. Exposure to chromium(VI) can cause cancer in the digestive tract and lungs, epigastric pain, nausea, severe diarrhea, vomiting, and hemorrhage [7]. Although chromium can access many oxidation states, chromium(VI) and chromium(III) are the species that are mainly found in industrial effluents [8]. Chromium(VI) is more toxic than chromium(III) and is of more concern [9]. Various methods have been developed to remove heavy metal ions, i.e. coagulation and precipitation, ion exchange treatment, membrane filtration, adsorption and electrochemical technique, but limited success has been achieved to date because of their less efficacy. Adsorption is one of the most promising heavy metals removal strategies because of its low cost, ease of operation, and lack of secondary pollution. Hydrogels have recently attracted a lot of attention because they can be utilized as a preferred adsorbent for extracting heavy metal ions from wastewater.

With the increase of surface area effectiveness of hydrogels increase. As submicrometer-sized hydrogel has an extremely large surface area than bulk hydrogel and can incorporate diverse functional groups into polymeric networks, it has attracted a lot of attention recently [10-13]. Submicrometer-sized hydrogel particles can be used in heavy metal removal, dye removal, waste water treatment, drug delivery, contact lens, biosensor, tissue engineering, food industry and so on.

1.1 Heavy metal removal techniques

Heavy metal is a serious problem nowadays. These heavy metals are discharged into water from various chemical industries, tanneries, mines, and other sources. They are harmful to living organisms. So, it is necessary to eliminate these heavy metals to minimize the risk of uptake by plants, animals, and humans. In the last few decades, several methods have been developed and extensively investigated for heavy metal removal. There are several methods for heavy metal removal: chemical precipitation, adsorption, ion exchange, membrane filtration, coagulation-flocculation, and floatation [14].

1.1.1 Chemical precipitation method

Chemical precipitation is effective and the most widely used process in industry [15] because it is relatively simple and inexpensive to operate. In precipitation processes, chemicals react with heavy metal ions to form insoluble precipitates. The forming precipitates can be separated from the water by sedimentation or filtration, and the treated water is then drained and appropriately discharged or reused. The chemical precipitation processes include hydroxide precipitation, sulfide precipitation, heavy metal chelating precipitation, etc.

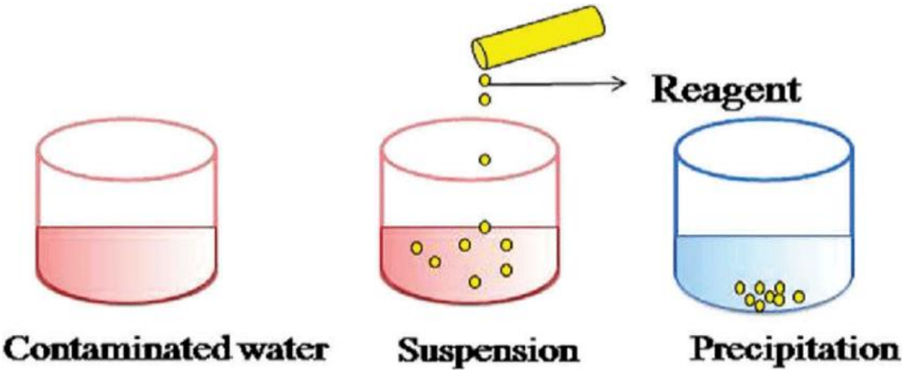

Figure 1.1.1. Schematic diagram showing chemical precipitation for removal of heavy metal ions [16].

1.1.2 Hydroxide precipitation method

The most widely used chemical precipitation technique is hydroxide precipitation because of its relative simplicity, low cost, and ease of pH control [17]. The solubilities of the various metal hydroxides are minimized in the pH range of 8.0 to 11.0. The metal hydroxides can be removed by flocculation and sedimentation. A variety of hydroxides have been used to precipitate metals from wastewater, based on the low cost and ease of handling. Lime is the preferred choice of base used in hydroxide precipitation in industrial settings.

1.1.3 Sulfide precipitation method

Sulfide precipitation is also an effective process for the treatment of toxic heavy metals ions. One of the primary advantages of using sulfides is that the solubilities of the metal sulfide precipitates are dramatically lower than hydroxide precipitates. Sulfide precipitates are not amphoteric, and hence, the sulfide precipitation process can achieve a high degree of metal removal over a broad pH range compared with hydroxide precipitation.

1.1.4 Heavy metal-chelating precipitation method

In conventional chemical precipitation processes to treat the heavy metal wastewaters have many limitations, and it is challenging to meet the increasingly stringent environmental regulations by application of traditional precipitation processes. As an alternative, many companies use chelating precipitants to precipitate heavy metals from aqueous systems. Matlock et al [18]. designed and synthesized a new thiol-based compound, 1,3benzenediamidoethanethiol di-anion (BDET2-). BDET2- can effectively precipitate mercury in the chelate solution and heavy metals from acid mine drainage. Fu et al. [19] employed dithiocarbamate-type supramolecular heavy metal precipitants, *N*,*N*-bis(dithiocarboxy)piperazine (BDP) and 1,3,5-hexahydrotriazinedithiocarbamate (HTDC) to treat complex heavy metals from wastewater. It is observed that both BDP and HTDC could effectively reduce heavy metal ions in wastewater as much lower as 0.5 mg/L.

1.1.5 Ion exchange method

Ion-exchange processes have been widely used to remove heavy metals from wastewater due to their many advantages, such as high removal efficiency, high treatment capacity, and fast kinetics. Ion-exchange resin, either synthetic or natural solid resin, has the specific ability to exchange its cations with the metals in the wastewater. Besides synthetic resins, natural zeolites, naturally occurring silicate minerals, have been widely used to remove heavy metals from aqueous solutions due to their low cost and high abundance. Many researchers have demonstrated that zeolites exhibit good cation-exchange capacities for heavy metal ions under different conditions.

Clinoptilolite is one of the most frequently studied natural zeolites that have received extensive attention due to its selectivity for heavy metals. Recently, some researchers reported that the surface of clinoptilolite loaded with amorphous Fe-oxide species would significantly improve the exchange capacity of clinoptilolite [20] employed clinoptilolite-Fe system to simultaneously remove Cu, Mn, and Zn from drinking water. The system has a very large metal adsorption capacity, and for most cases, the treated water samples were suitable for human consumption or agricultural use.

1.1.6 Membrane filtration method

Membrane filtration technologies with different types of membranes show great promise for heavy metal removal due to their high efficiency, easy operation, and space-saving. The membrane processes used to remove metals from the wastewater are ultrafiltration, reverse osmosis, nanofiltration, and electro-dialysis methods.

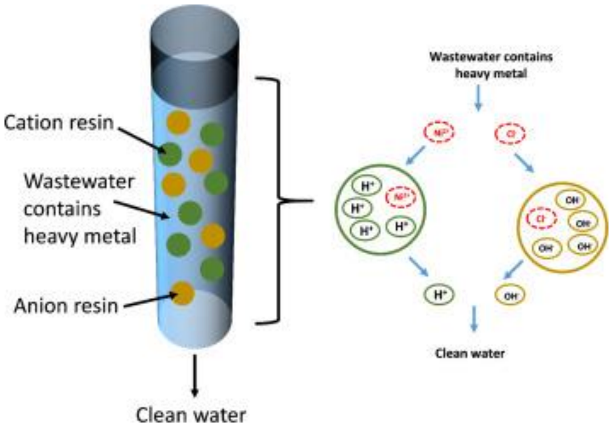

Figure 1.1.2 Adsorptive membranes for heavy metals removal from water [21]

1.1.7 Ultrafiltration method

Ultrafiltration (UF) is a membrane technique working at low trans-membrane pressures to remove dissolved and colloidal material. Since the pore sizes of UF membranes are larger than dissolved metal ions in the form of hydrated ions or as low molecular weight complexes, these ions would pass easily through UF membranes. Micellar enhanced ultrafiltration (MEUF) and polymer enhanced ultrafiltration (PEUF) were proposed to obtain high removal efficiency of metal ions. There is a lot of investigation on this topic, but not yet been utilized widely in the industry.

1.1.8 Reverse osmosis method

The reverse osmosis (RO) process uses a semi-permeable membrane, allowing the fluid that is being purified to pass through it while rejecting the contaminants. RO is one of the techniques which can remove a wide range of dissolved species from water. It accounts for more than 20% of the world's desalination capacity. It is an increasingly popular wastewater treatment option in chemical and environmental engineering. The RO process successfully removed $Cu^{2+}$and Ni^{2+} ions, and the rejection efficiency of the two ions increased up to 99.5% by using Na_2EDTA. This process applied a pilot-scale membrane bioreactor system combined with RO, and they found very high heavy metal removal efficiencies. The major drawback of RO is the high power consumption due to the pumping pressures and the restoration of the membranes.

1.1.9 Nanofiltration method

Nanofiltration (NF) is the intermediate process between UF and RO. NF is a promising technology for rejecting heavy metal ions such as nickel, chromium, copper, and arsenic from wastewater. NF process benefits from ease of operation, reliability, comparatively low energy consumption, and high efficiency of pollutant removal.

1.1.10 Electrodialysis method

Electrodialysis (ED) is another membrane process for separating ions across charged membranes from one solution to another using an electric field as the driving force. In most ED processes, ion-exchange membranes are used. The membranes are actually of two basic types: cation-exchange and anion-exchange membranes. This process has been widely used to produce drinking and process water from brackish water and seawater, treatment of industrial effluents, recovery of useful materials from effluents, and salt production. The process performed a new working system to investigate the removal of hexavalent chromium ions using a built-in ED pilot plant comprising a set of ion-exchange membranes.

1.1.11 Coagulation and flocculation method

Coagulation and flocculation followed by sedimentation and filtration are also employed to remove heavy metal from wastewaters. Coagulation is the destabilization of colloids by neutralizing the forces that keep them apart. Many coagulants are widely used in the conventional wastewater treatment processes such as aluminum, ferrous sulfate and ferric chloride, resulting in the effective removal of wastewater particulates and impurities by charge neutralization of particles and by enmeshment of the impurities on the formed amorphous metal hydroxide precipitates. The removal of heavy metal by coagulation of combined sewer overflows with two commercial coagulants, a ferric chloride solution and a polyaluminum chloride (PAC). Excellent heavy metal elimination was achieved within a narrow range of coagulants around optimum coagulant concentrations.

1.1.13 Electrochemical treatment method

Electrochemical methods involve the plating-out of metal ions on a cathode surface and can recover metals in the elemental metal state. Electrochemical wastewater technologies involve relatively large capital investment and an expensive electricity supply, so they haven’t been widely used. However, with the stringent environmental regulations regarding wastewater discharge, electrochemical technologies have regained their importance worldwide during the past two decades. For instance, electrocoagulation (EC), electro flotation, and electrodeposition methods. EC involves generating coagulants in situ by dissolving either aluminum or iron ions from aluminum or iron electrodes. The metal ion generation takes place at the anode, and hydrogen gas is released from the cathode. The hydrogen gas can help to float the flocculated particles out of the water. Heidmann and Calmano [20] studied the performance of an EC system with aluminum electrodes for removing Zn^{2+}, Cu^{2+}, Ni^{2+}, $Ag^{+,}$ and $Cr_2O_7^{2-}$. Electrochemical heavy metal wastewater treatment techniques are regarded as rapid and well-controlled that require fewer chemicals, provide good reduction yields and produce less sludge. However, electrochemical technologies involving high initial capital investment and the expensive electricity supply restricts its development.

1.1.14 Adsorption method

Adsorption is now recognized as an effective and economical method for heavy metal wastewater treatment. The adsorption process is widely used to remove heavy metals from wastewater because of its low cost, availability, and eco-friendly nature. The adsorption process offers flexibility in design and operation, and many cases will produce high-quality treated effluent. In addition, as adsorption is sometimes reversible, adsorbents can be regenerated by a suitable desorption process. Both commercial adsorbents and bio-adsorbents are used to remove heavy metals from wastewater, with high removal capacity.

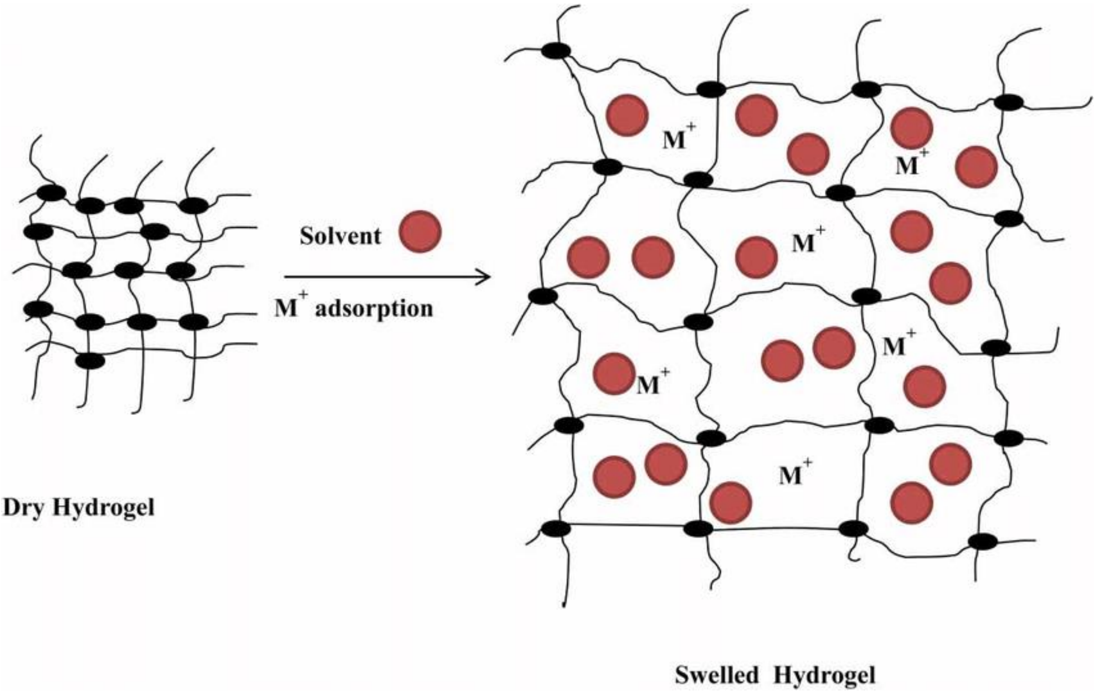

Figure 1.1.3 Hydrogel adsorption mechanism [23]

During the last decade, hydrogels have been used as potential adsorbents for the removal of contaminants from aqueous solutions. To improve adsorption efficiency, numerous different particles can be chosen to encapsulate into hydrogels, and each particle has its respective advantages. Depending on the type of pollutants and approaching method, the particles will be used to prepare hydrogels. The hydrogels commonly applied in water/wastewater treatment were mainly classified into three classes according to their shape: hydrogel beads, hydrogel films, and hydrogel nanocomposites [24].

1.2 Hydrogel

A crosslinked hydrophilic polymer that does not dissolve in water is referred to as a hydrogel. They are extremely absorbent while still retaining well-defined shapes. Smart hydrogels are well-defined three-dimensional polymer networks with the ability to dramatically change their volume and properties by absorbing a large amount of water in response to change in environmental stimuli such as temperature, pH, ionic strength, pressure, solvent, and electric or magnetic fields [25-26]. The ability of hydrogels to absorb water arises from hydrophilic functional groups attached to the polymer backbone. They have received considerable attention in the past 50 years due to their exceptional promise in a wide range of applications [27-28]. Hydrogel also possesses a degree of flexibility very similar to natural tissue due to its large water content. The water inside the hydrogels allows free diffusion of some solute molecules, while the polymers serve as a matrix to hold water together. They usually exhibit simultaneously liquid-like and solid-like properties, which causes interesting relaxation behavior. Hydrogels may exhibit drastic volume changes in response to specific external stimuli such as pH, temperature, solvent, electric field, magnetic field, antigen, antibody, and so on [29]. During the last two decades, natural hydrogels were gradually replaced by synthetic hydrogels with long service life, high water absorption capacity, and high strength. Synthetic polymers usually have a well-defined structure that can be modified to yield tailor ability, degradability, and functionality. Hydrogels can be synthesized from purely synthetic components that are stable in the conditions of sharp and strong temperatures fluctuations [30].

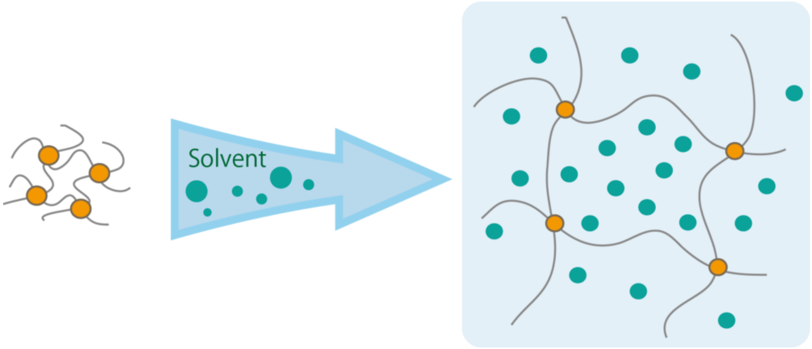

Figure 1.2 The schematic diagram of the network structure of gel, swelling when immersed into a solvent [25].

Hydrogels may be synthesized in many ways, including one-step procedures like polymerization and parallel cross-linking of multifunctional monomers, multiple-step procedures involving synthesis of polymer molecules having reactive groups and their subsequent cross-linking, and by reacting polymers with suitable cross-linking agents. Crosslinking can be initiated by heat, pressure, change in pH, or radiation. Cross-linkers are chosen depending on the chemical specificity and availability of different reactive groups. The polymer engineer can design and synthesize polymer networks from a molecular-scale control over macrostructure to obtain biodegradability, mechanical strength, and chemical and biological response to stimuli [31].

Hydrogels are used in drug delivery, heavy metal removal, image enhancement, remote-controlled actuators and valves, bone marrow regeneration, separation technology, tissue engineering, chemical, and bio-sensing, etc. [28-29]. Hydrogels can sustain high compressions, resist slicing and withstand high levels of deformation, such as bending, twisting, and stretching for their rapid stimuli-responsive characteristics and highly elastic properties [32]. Hydrogels can be classified into two categories based on the cross-link junctions. Physical networks have transient junctions that arise from either polymer chain entanglements or physical interactions, and chemically cross-linked networks have permanent junctions [33].

1.2.1 Physically crosslinked hydrogel

Physical crosslinks include entanglement of polymer chains, hydrogen bonding, hydrophobic interaction, and crystallite formation. These physical crosslinks may not be permanent in nature, but they are sufficient to make hydrogels insoluble in an aqueous media. Physical crosslinking gives reversible hydrogels having inhomogeneities or network defects due to the presence of free chain ends or chain loops. Physically crosslinked hydrogels are usually synthesized by ionic interaction, crystallization, stereo complex formation, hydrophobic interaction, protein interaction, hydrogen bonding, and so on. In ionic interactions, hydrogels can be crosslinked under mild conditions at room temperature and physiological pH. This process of cross-linking does not require the presence of ionic groups in the polymer chains. The use of metallic ions can yield a more robust hydrogel. For stereo complex formation, a hydrogel is formed through crosslinking between the acid of natural oligomers of opposite chirality.

1.2.2 Chemically crosslinked hydrogel:

Chemically crosslinked hydrogels are formed by the covalent crosslinking of polymers. One common way to create a covalently crosslinked network is to polymerize end-functionalized macromers. Hydrogels are crosslinked with many compounds such as glutaraldehyde [34], formaldehyde, epoxy and di-aldehyde [35-37]. A net-like structure along with void imperfections enhances the hydrogel's ability to absorb large amounts of water. The type and degree of crosslinking influence many of the network properties, including swelling properties, elastic modulus, and transport of molecules [38]. Chemically cross-linked hydrogels are synthesized by chain-growth polymerization, addition polymerization, condensation polymerization, and gamma and electron beam polymerization.

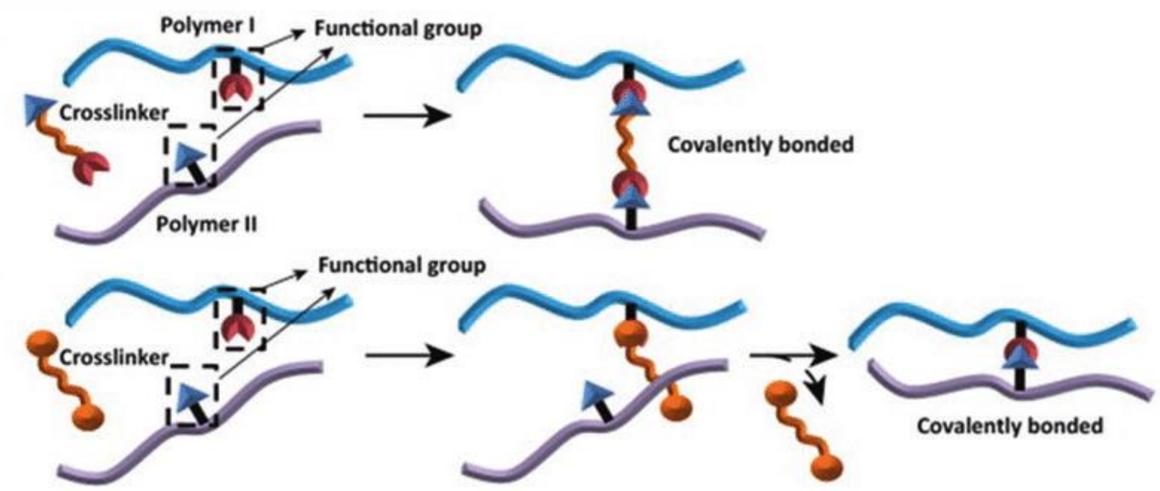

Fig. 1.2.1 Schematic representation of the formation of chemically cross-linked hydrogels [39]

Chain-growth polymerization includes free radical polymerization, controlled free radical polymerization, anionic and cationic polymerization. It is done by three processes viz., initiation, propagation, and termination. After initiation, a free radical active site is generated, which attacks monomers in a chain link-like fashion.

1.3 Stimuli-responsive hydrogels

Hydrogels that respond to external stimuli are known as stimuli-responsive hydrogels. Typical stimuli are temperature [40-43], pH [45,46], electric field [46], light [47,48], magnetic field [49], concentration of electrolytes or glucose etc. The following changes of the hydrogels, for example, isolation/precipitation, degradation, drug release, change in hydration state, swelling/shrinking, hydrophilic/hydrophobic surface, change in shape, conformational change, and micellization, are usually affected by external stimuli [50,51].

1.3.1 Thermo-responsive hydrogel

Thermo-responsive hydrogels are sensitive to temperature and change their microstructural features in response to change in temperature. These hydrogels belong to the class of stimuli-responsive hydrogels and are also capable of changing their physical properties rapidly with changing the environmental temperature [52-53]. Thermo-responsive hydrogels exhibit a volume phase transition at a certain temperature which causes a sudden change in the solvation state. Polymers that become insoluble upon heating have a so-called lower critical solution temperature (LCST). Systems that become soluble upon heating have an upper critical solution temperature (UCST). LCST and UCST systems are not restricted to an aqueous environment. However, only the aqueous systems are of interest for biomedical applications. Some systems exhibit both LCST and UCST behavior, but that is usually not occurring within the setting of the intended biomedical applications [54].

Typical LCST polymers are formed from *N*-isopropylacrylamide (NIPAm) [55,56], *N*,*N*-diethylacrylamide (DEAM) [57], methylvinylether (MVE) [58,59], *N*-vinylcaprolactam (NVCl), and so on [60,61] as monomers. On the other hand, typical UCST system is formed by a combination of two monomers for instance acrylamide (AAm) and acrylic acid (AAc) [62].

1.3.2 Magneto- responsive hydrogel

Magnetic responsive materials are the topic of intense research interest due to their potential applications in the biomedical, coatings, microfluidics and microelectronics fields [63]. Magneto responsive membranes are of special interest as they can realize spatial, temporal, and remote control and have great potential in microfluidic systems for analytical or therapeutic devices [64-66]. As there are very few intrinsically magneto-responsive polymers, most magneto responsive materials are composite materials consisting of inorganic magnetic nano particles (MNP) with magnetic orientation [67-69] or magnetic heating and another polymeric component as the actuator. Magneto-responsive membranes can be classified into two types: nanoactuator and nano-heater. One good example of such design is a nanofiltration membrane with micro-mixers on its surface introduced by Himstedt et al. [70]. The nano-heater type utilizes the heating effect of MNP under high temperature usually, the systems are combined with thermo synergistic effect of the two components.

1.3.3 pH-responsive hydrogel

pH-responsive polymers swell or collapse depending on the pH of their environment. This behavior is exhibited due to the presence of certain functional groups in the polymer chain. The ionic pH-sensitive polymers can accept or release protons in response to pH changes [71]. These polymers contain acid groups (carboxylic or sulfonic) or basic groups (ammonium salts). In other words, pH-sensitive polymers are polyelectrolytes that have in their structure acid or basic groups that can accept or release protons in response to pH changes in the surrounding environment. This smart polymer changes its solubility by changing the electrical charge of the polymer molecule. Thus, the transition from a soluble state to an insoluble state is caused by the decrease of the electrical charge in the polymeric molecules. The polymer's electric charge can be decreased by decreasing its pH via neutralizing the electric charge and reducing the hydrophilicity (increasing hydrophobicity) of the polymeric macromolecules.

1.3.4 Light sensitive hydrogel

Light-sensitive hydrogels have potential applications in developing optical switches, display units, and ophthalmic drug delivery devices. They can serve as functional materials with potential applications in the areas of drug/gene delivery, photography, paints/coatings, sensors, and so forth [72]. Azobenzene and its derivatives have a unique light-induced trans-cis isomerization property [73]. Irradiating azobenzene units with light causes them to isomerize from the more stable trans configuration to the less stable cis configuration. Thus, they have been used as light-responsive units in many gel systems in which the sol-to-gel or gel-to-sol phase transition of the gel systems is controlled by light-induced trans-cis isomerization of the azobenzene units. A host-guest chemistry approach is also advantageous for producing light-responsive hydrogels. Cyclodextrins

(CDs) and their derivatives acting as hosts can form supramolecular inclusion complexes with a series of guests in which the guest molecules are included within the hydrophobic inner cavities of the CDs [74].

1.3.5 Electric field sensitive hydrogel

Although many materials that deliver drugs in response to ultrasound, light, and magnetic signals have been developed, activating these materials typically requires large or specialized equipment. Electrical signals, on the other hand, are easy to generate and control. Electric stimuli have been successfully utilized to trigger the release of molecules via conducting polymeric bulk materials or implantable electronic delivery devices [75-77].

1.3.6 Multi-stimuli responsive hydrogel

Responsive polymer hydrogels can largely and reversibly change their volume or shapes under slight external stimuli, including temperature, pH, ionic strength, special chemicals, redox, light, humidity, electric field, magnetic fields, etc. This property of responsive polymer hydrogels can be utilized in diverse applications, such as sensors, valves, on-off switches, biomimetic actuators, artificial muscles, and so on. A variety of stimuli-responsive hydrogels has been emerging recently by putting this smart hydrogel into more than one responsiveness. 1.2.7 pH- and thermo-responsive hydrogel Stimuli-responsive polymers mimic biological systems in a crude way where an external stimulus (e.g., pH or temperature) results in a change in properties, including change in conformation, change in solubility, alteration of the hydrophilic/ hydrophobic balance or release of a bioactive molecule (e.g., drug molecule). To obtain a temperature and pH-sensitive polymer, it is only necessary to combine temperature-sensitive monomers.

1.3.8 Magneto and thermo-responsive hydrogel

Dual temperature and magnetic responsive hydrogels are the most widely investigated because these two stimuli are easy to apply. Poly(*N*-isopropylacrylamide) is the popular temperature-responsive hydrogel due to its volume phase transition temperature (around 32◦C) close to normal body temperature.

Magnetic property is very important poperies of any materials for separation and many other purposes. Fe_3O_4 and Ni nanoparticles are usually used as magnetic particles. If a magnetic particle is incorporated with any temperature-responsive polymer network, the hydrogel will respond with the temperature and magnetic field change. Magneto and thermo-responsive hydrogel can be used in drug delivery, heavy metal removal electronics devices and so on.

1.4 Biocompatibility of hydrogel

Biocompatibility is a field that first attracted the attention of researchers in the 1940s in the context of medical implants and their beneficial and harmful interactions with the body. In 1987, the biocompatibility was formally defined as “the ability of a biomaterial to perform with an appropriate host response in the specific application”. Biocompatibility is a very important property of hydrogel for use in biomedical and tissue engineering fields. The goal of evaluating the biocompatibility of any material is to determine any toxic effects on the body. Therefore, a biomaterial must be assessed to determine the biological responses which could cause damage or unwanted side effects to the host. The biocompatibility of the hydrogels was evaluated to assess their potential as a drug carrier.

1.5 Nanocomposite Hydrogels (NCHGs)

Nanocomposite hydrogels are nanomaterial’s (metals, non-metals, metal oxide, and polymeric moieties) filled, hydrated, polymeric networks that exhibit superior functionality to traditionally made hydrogels. By controlling the interaction between nanoparticles and polymer chains, a range of physical, chemical, and biological properties can be engineered [79] and applied in diverse fields, including catalysis, electronics, bio-sensing, drug delivery, nano-medicine, and environmental remediation. Properties imparted to the composites depend on the type of nanoparticles incorporated, which in turn is determined by the proposed application of the designed composite. Different types of nanocomposite hydrogels and their associated properties are described below.

1.5.1. Metal Nanocomposite

Various types of metal nanoparticles such as Ag, Au, Cu, Fe-Co bimetallic, Co-Ni bimetallic and Pt have been used as nanofiller (incorporated in the hydrogels) in the nanocomposite hydrogels. These metallic nanoparticles incorporated nanocomposite hydrogels show unique properties, including excellent antibacterial activity, optical properties, electrical conductivity, hydrogenation catalysis, and waste removal application. Platinum (Pt) metal is well known as a hydrogenation catalyst. Platinum nanocomposite hydrogels (PtNCHGs) were found to be an efficient catalyst for the hydrogenation of *p*-nitroaniline [80]. Magnetic NPs of cobalt (Co) or nickel (Ni) have been incorporated into hydrogels to form soft magnetic field-driven actuators for muscle-like application [81]. Cu has been investigated as a cost-effective alternative to

AgNPs and AuNPs antimicrobial agents [82]. Fe-Co bimetallic NPs synthesized in PAAM hydrogel network to form magnetic hydrogels for waste removal application [83].

1.5.2 Metal oxide Nanocomposite

Hydrogels Iron oxide (Fe_xO_y) is a commonly synthesized ferromagnetic material that has been incorporated into hydrogels to form ferrogels [84]. Ferrogels are effective absorbents for toxic ions such as lead (Pb^{2+}), chromium (Cr^{2+}) and arsenic (As^{5+}). [85].

1.5.3 Non-Metal Nanocomposite

Hydrogels Carbon-based materials (graphene oxide, nanodots, nanotubes), quantum dots, and Si have been used to create composite hydrogel materials with unique properties and functions which are nonmetal based NCHGs. Si-NCHGs have been used as a support for catalysts or functional materials. Alvarez and co-workers developed antibiotic-loaded (gentamicin) SiNCHGs that exhibited prolonged antibacterial activity and increased mechanical strength [86]. Carbon nanotubes [87]; graphene oxide [88], and even melanin [89] when placed in hydrogels act as NIR light absorbing materials which are useful for photothermal drug delivery.

1.5.4 Polymeric Nanocomposite

Hydrogels Polymeric nanoparticles composed of micelles [90], nanogels [91], core-shell particles [92] dendrimers [93], hyperbranched polymers, and liposomes have been developed for a variety of applications. The use of polymeric NPs for reinforcement of hydrogels is not restricted to biomedical applications. Polystyrene (PS), a material commonly used for packaging and storage, could be used as filler in hydrogels to impart mechanical strength [94].

1.6 Nanoparticles (NPs)

The particles which have at least one of the dimensions in 1-100 nm range is called nanoparticles (NPs). With the decrease in the dimensions of the materials to the nano level, their properties change. The NPs possess unique physicochemical, optical, and biological properties which can be manipulated suitably for desired applications [95]. Moreover, as the biological processes also occur at the nano scale and due to their amenability to biological functionalization, the NPs are finding important applications in the field of medicine [96]. The NP is broadly grouped into organic NP and inorganic NP.

Nanoparticles can be classified into different types according to their size, morphology, physical and chemical properties. Some of them are carbon-based nanoparticles, ceramic nanoparticles, metal nanoparticles, semiconductor nanoparticles, polymeric nanoparticles and lipid-based nanoparticles. Nanoparticles are synthesized due to the reduction of material dimensions, which have a remarkable effect on their characteristics that significantly vary from their corresponding starting bulk materials. Nanoparticles possess these significant properties due to - a.) large surface atom b.) large surface energy c.) spatial confinements and d.) reduced imperfections [97].

1.7 Properties of nanoparticles

1.7.1 Optical Properties:

Metal nanoparticles show different optical properties as compared to their starting bulk materials form. It also depends on their composition shape, size and the surrounding medium. The optical properties of nanoparticles vary from the visible region based on the size and shape of the nanoparticles. This is due to the interaction of electron clouds that are present on the surface of metal nanoparticles with electromagnetic radiation. Some metal nanoparticles (such as gold, silver and copper) are known to have specific unique optical properties within a certain size limit of particles in the visible and in the NIR region [98].

1.7.2 Magnetic properties

At the nano range, the magnetic properties of different nanoparticles differ from that of starting bulk material. At the nano level, ferromagnetic properties form a single domain with large single magnetic moments. These will also change the magnetic properties drastically. At the thermodynamic equilibrium state magnetization behavior of nanoparticles is similar to that of atomic magnetization, but with a large magnetic moment. At a certain nanoscale level, ferromagnetic particles become superparamagnetic.

Magnetic nanoparticles are a class of nanoparticle that can be manipulated using magnetic fields. Such particles commonly consist of two components, a magnetic material, often iron, nickel, and cobalt, and a chemical component that has functionality. While nanoparticles are smaller than 1 micrometer in diameter (typically 1–100 nanometers), the larger microbeads are 0.5–500 micrometer in diameter. Magnetic nanoparticle clusters that are composed of a number of individual magnetic nanoparticles are known as magnetic nanobeads with a diameter of 50–

200 nanometers. Magnetic nanoparticle clusters are a basis for their further magnetic assembly into magnetic nano chains. The magnetic nanoparticles have been the focus of much research recently because they possess attractive properties which could see potential use in catalysis including nanomaterial-based catalysts, biomedicine and tissue-specific targeting, magnetically tunable colloidal photonic crystals, microfluidics, magnetic resonance imaging, magnetic particle imaging, data storage, environmental remediation, nanofluids, optical filters, defect sensor, magnetic cooling and cation sensors. The physical and chemical properties of magnetic nanoparticles largely depend on the synthesis method and chemical structure. In most cases, the particles range from 1 to 100 nm in size and may display superparamagnetism [99].

1.7.3 Surface Plasmon Resonance (SPR)

On the surface of nanoparticles large numbers of atoms are found, which forms electron clouds on their surface. This free electron causes a dipole excitation under the electric field vector of the incoming light due to the dipole excitation across the particles. These electrical charges act as a restoring force and bring back electron clouds to their original position, thus causing the oscillations of the electron cloud. So that the electron density within the surface layer vibrates; however, the density in the interior part of the particles remains constant. This phenomenon is known as surface plasmon resonance which is explained by Mie in 1908 based on Maxwell's equation of scattering [99].

1.7.4 Thermal properties

It is found that metal and semiconductor nanoparticles have a remarkably lower melting point or low transition temperature than their bulk form. It is found that when the particles size is below 100 nm the melting point of the particle is lowered and it is allocated to increase in their surface energy with a reduction of the size of nanoparticles. As the phase transition temperature is declining this can be led to the changes in the surface energy to volume energy as a function of size [100].

1.7.5 Mechanical properties

As the size of the particle decreases the mechanical properties of nanomaterials increases. Most of the studies have been carried on the mechanical properties of one-dimensional structures such as nanowires. The mechanical strength of nanowires or nanorods is enhanced, which is attributed to the high internal perfection of the nanowires. Generally, imperfections such as dislocation, micro-twins' impurities etc. in crystals are highly energetic and should be eliminated from the correct crystal structures. The smaller the cross-section of nanowires, the probability of a finding of imperfection as nanoscale diameter should be less as dimension makes the elimination of such imperfections possible.

1.8 Polymerization

A polymer is a substance that is made up of very large molecules that are made up of many repeating units called monomers. Polymerization is a process of reacting a large number of monomer molecules together in a chemical reaction to form polymer chains or three-dimensional networks. The macromolecules produced from a polymerization may have a linear or a branched structure or the shape of a complex and three-dimensional network. [101-103]
Polymerization can occur via a variety of reaction mechanisms that depend on the complexity of monomers due to the variety of functional groups [103]. Based on origin, polymers are two types: synthetic and natural. Natural polymers occur in nature and can be extracted. They are often water-based. Examples of naturally occurring polymers are silk, wool, DNA, cellulose and proteins. Synthetic polymers are long-chain molecules possessing uniform repeat monomers. The chains can have different lengths. Polymers have interesting physical and chemical properties because of the length of the chain. Examples of synthetic polymers include nylon, polyethylene, polyester, Teflon, and epoxy. Low density versus strength is one of the most useful and interesting properties of polymers. [104]

1.9 Polymerization technique

There are various polymerization techniques for the formation of polymers. : Bulk, emulsion, suspension, solution.

1.9.1 Bulk Polymerization:

By adding a soluble initiator with a pure monomer in the liquid state, bulk polymerization or mass polymerization is carried out. The initiator should dissolve in the monomer, and the reaction is initiated by heating or exposure to radiation. As the reaction proceeds, the mixture becomes more viscous, the reaction is exothermic, and a wide range of molecular masses are produced. This process can be used for Free radical polymerizations and some step-growth or condensation polymerization.

The main advantage of this method is the product of polymerization obtained from this type of process is the purest form of polymer, and the greatest yield of polymer per unit volume. Bulk polymerization has some advantages; the polymer obtained is pure, molecular weight distribution can be easily changed using a chain transfer agent, the product obtained has high optical clarity, and so on. The main disadvantage of this method is that as the medium gets viscous, the diffusion of the growing polymer chain becomes restricted, collisions become less, and thereby termination becomes difficult. Due to active radical sites accumulation, the rate of polymerization increases enormously, and sometimes, the uncontrolled exothermic reactions can lead to an explosion.

1.9.2 Suspension Polymerization

In a typical suspension polymerization system, one or more water-insoluble monomers containing oil-soluble initiators are dispersed in the continuous aqueous phase. A combination of strong stirring and small amounts of suspending agents (stabilizers) are used. Suitable conditions of mechanical agitation are maintained through the whole polymerization process [105-107]. To control the enormous amount of heat release in bulk polymerization, suspension polymerization method was developed. This technique can polymerize only water-insoluble monomers. Since each monomer droplets are isolated and independent of other droplets, each of these droplets acts as a tiny bulk reactor. Heat transfer occurs from the droplets to the water having a large heat capacity and low viscosity. As the entire bulk of the monomer is divided into innumerable tiny droplets, control of the kinetic chain length of the polymer is also quite good, so the product has a narrow molecular weight distribution.

The advantages of the method are better heat control of the reaction, and separation is much easier than in solution polymerization. The disadvantage is that few monomers are water-soluble.

1.9.3 Solution Polymerization:

In this process, the monomer is dissolved in a suitable inert solvent along with the chain transfer agents wherever used. The free radical initiator is also dissolved in the solvent medium, whereas ionic and coordination catalysts can be dissolved or suspended. The solvent enhances the heat capacity, thereby reducing the viscosity and promotes proper heat transfer. Solution polymerization techniques can advantageously be used where the polymer is used in solution form (as adhesive and coating compositions). Chain transfer to the solvent used cannot be ruled out; hence it is difficult to obtain very high molecular weight products. The polymer formed will also have to be isolated from the solution either by evaporation or precipitation in a non-solvent and removal of their final traces is always extremely difficult [108].

1.9.4 Emulsion polymerization:

Emulsion polymerization is a process of great industrial importance. It offers profound advantages over other polymerization processes due to its multiphase and compartmentalized nature. An emulsion polymerization system provides the possibility to yield a product with unique properties and performance characteristics. Researchers are interested in emulsion polymerization because it offers the possibility of producing products with special properties which are not easily produced by other types of polymerization processes. [109-111]

This is the most widely used method of polymerization. In emulsion polymerization, the monomer is dispersed in an aqueous phase as fine droplets, which are then stabilized by surface-active agents, protective colloids, and also by certain buffers. The surfactants can be cationic or non-ionic. Surfactants lower the surface tension at the monomer water interface and facilitate emulsification of the monomer in water. The surfactant will form micelles when their concentration exceeds critical micelle concentration (CMC), which are dispersed throughout the solution. In micelle formation, the emulsifier molecule aggregates so that the polar end of the molecule aligns themselves outward, and the hydrocarbon end comes close to each other at the interior. Due to the close proximity of the hydrocarbon ends of all emulsifier molecules, the interior of the micelle acts as a hydrocarbon phase.

When the monomer is added and agitated, emulsification takes place. The resultant emulsion is a complex system: A molecular solution of the emulsifier in water is the continuous phase wherein the monomer droplets, and micelle (having solubilized monomer at their interior) are uniformly dispersed. Polymerization techniques Emulsion systems generally utilize a water-soluble initiator as persulfate or hydrogen peroxide. With the more and more polymer formation, the polymer aggregates into fine particles and get surrounded and then stabilized by the emulsifier layer of the micelle. At the end of the polymerization, the fine particles of the polymer are stabilized by the emulsifier and dispersed uniformly in the aqueous layer [112-114].

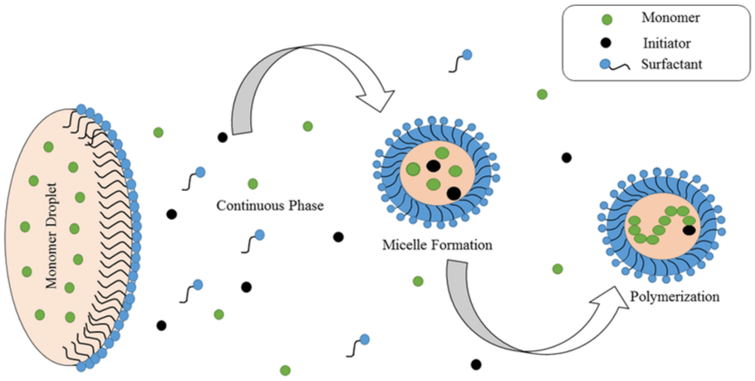

Figure 1.9.1 Schematic representation of Emulsion polymerization [111]

1.10 Research Goal:

Smart hydrogels are well-defined three-dimensional polymer networks with the ability to absorb large amounts of water in response to changes in environmental stimuli, allowing them to change their volume and properties dramatically. Although macro or bulk hydrogels have high potential in varieties of practical applications, submicrometer-sized hydrogels are faster in responding to change their size with environmental stimuli due to their extremely large relative surface area. Smart hydrogels can sustain high compressions, resist slicing and withstand a high level of deformation, such as bending, twisting and stretching for their rapid stimuli-responsive characteristics and highly elastic properties [115]. In separate investigations, different methods were employed to synthesis submicrometer-sized hydrogel particles with NIPAm as the main monomer because of its thermoresponsive and biodegradable nature [116-117].

The incorporation of magnetic nanoparticles into hydrogel systems will afford the hydrogel magnetism resulting in submicrometer-sized magnetic hydrogels. [118-119]. This characteristic will permit remote control or separation of the hydrogel from the solution. Magnetic hydrogels have attracted researchers' interest in recent years due to their dynamic features [120].

Various heavy metals with a prescribed limit are important for the human body while above the limit has adverse effects on health and the environment [121-122]. To remove toxic ionic species of heavy metal, various methods have been developed but limited success has been achieved to date because of their less efficacy [123-124].

The present study aims to prepare a temperature-sensitive magnetic submicrometer-sized hydrogel by emulsion polymerization of a thermo-sensitive monomer with an ionic comonomer and magnetic nano particle in presence of a suitable initiator and cross-linker. Different types of magnetic nano particles and co-monomer will be used to fabricate the hydrogels and their heavy metals removal capacity via electrostatic interactions will be studied in a systematic manner.

The main objectives with specific aims of the proposed research are

- Facile synthesis of different types of magnetic nanoparticles.
- Facile synthesis of different types of temperature-sensitive magnetic submicrometer-sized hydrogel particles.
- Removal of heavy metal from water using magnetic submicrometer-sized hydrogel particles.
- Separation of heavy metal containing submicrometer-sized hydrogel particles from the system by applying an external magnetic field.

References

[1] H. Ali, E. Khan, and I. Ilahi, “Environmental chemistry and ecotoxicology of hazardous heavy metals: Environmental persistence, toxicity, and bioaccumulation,” *Journal of Chemistry*, Vol. 2019, pp. 1-14 (2019).

[2] G. Aragay, J. Pons, and A. Merkoçi, “Recent trends in macro-, micro-, and nanomaterial-based tools and strategies for heavy-metal detection,” *Chemical Reviews*. Vol.111(5), pp. 3433–3458 (2011).

[3] W. S. Wan Ngah and M. A. K. M. Hanafiah, “Removal of heavy metal ions from wastewater by chemically modified plant wastes as adsorbents: A review,” *Bioresource Technology*, Vol. 99(10), pp. 3935–3948 (2008).

[4] R. Singh, N. Gautam, A. Mishra, and R. Gupta, “Heavy metals and living systems: An overview,” *Indian Journal of Pharmacology*, Vol. 43(3), pp. 246-253 (2011).

[5] L. Järup, “Hazards of heavy metal contamination,” *British Medical Bulletin*, Vol. 68, pp. 167–182 (2003).

[6] J. Barnhart, “Occurrences, Uses, and Properties of Chromium,” *Regul. Toxicol. Pharmacol.*, Vol. 26, pp.S3-S7 (1997).

[7] K. Mohanty, M. Jha, B. C. Meikap, and M. N. Biswas, “Removal of chromium (VI) from dilute aqueous solutions by activated carbon developed from Terminalia arjuna nuts activated with zinc chloride,” *Chem. Eng. Sci.*, Vol. 60, pp. 3049-3059 (2005).

[8] D. Mohan and C. U. Pittman, “Activated carbons and low-cost adsorbents for remediation of tri- and hexavalent chromium from water,” *Journal of Hazardous Materials*, Vol. 137, pp. 762-811 (2006).

[9] Z. A. AL-Othman, R. Ali, and M. Naushad, “Hexavalent chromium removal from aqueous medium by activated carbon prepared from peanut shell: Adsorption kinetics, equilibrium and thermodynamic studies,” *Chem. Eng. J.*, Vol. 184, pp. 238-247 (2012).

[10] A. Vijayalakshmi, D. L. Arockiasamy, A. Nagendran, and D. Mohan, “Separation of proteins and toxic heavy metal ions from aqueous solution by CA/PC blend ultrafiltration membranes,” *Sep. Purif. Technol.*, Vol. 62, pp. 32-38 (2008).

[11] C. A. Basha, M. Somasundaram, T. Kannadasan, and C. W. Lee, “Heavy metals removal from copper smelting effluent using electrochemical filter press cells,” *Chem. Eng. J.*, Vol. 171, pp. 563-571 (2011).

[12] L. Charerntanyarak, “Heavy metals removal by chemical coagulation and precipitation,” in *Water Science and Technology*, Vol. 39, pp. 135-138 (1999).

[13] A. Dąbrowski, Z. Hubicki, P. Podkościelny, and E. Robens, “Selective removal of the heavy metal ions from waters and industrial wastewaters by ion-exchange method,” *Chemosphere*. Vol. 56, pp. 91-106 (2004).

[14] K. Singh, N. A. Renu, and M. Agarwal, “Methodologies for removal of heavy metal ions from wastewater: an overview,” *Interdiscip. Environ. Rev.*, Vol. 18(2), pp. 124 (2017).

[15] Y. Ku and I.-L. Jung, “Photocatalytic reduction of Cr (VI) in aqueous solutions by UV irradiation with the presence of titanium dioxide,” *Water Research,* Vol. 35, pp. 135-142 (2001).

[16] R. Chakraborty, A. Asthana, A. K. Singh, B. Jain, and A. B. H. Susan, “Adsorption of heavy metal ions by various low-cost adsorbents: a review,” *International Journal of Environmental Analytical Chemistry*. Vol. 12, pp. 1-38 (2020).

[17] J. L. Huisman, G. Schouten and C. Schultz, “Biologically produced sulfide for purification of process streams, effluent treatment and recovery of metals in the metal and mining industry,” *Hydrometallurgy*, Vol. 83, pp. 106-113 (2006).

[18] M. M. Matlock, B. S. Howerton and M. A. Van Aelstyn, “Advanced Mercury Removal from Gold Leachate Solutions Prior to Gold and Silver Extraction: A Field Study from an Active Gold Mine in Peru,” *Environmental Science & Technology,* Vol. 36, pp. 1636-1639 (2002).

[19] F. Fu, R. Chen and Y. Xiong, “Application of a novel strategy—Coordination polymerization precipitation to the treatment of Cu2+-containing wastewaters,” *Separation and Purification Technology*, Vol. 52, pp. 388-393 (2006).

[20] M. K. Doula, “Simultaneous removal of Cu, Mn and Zn from drinking water with the use of clinoptilolite and its Fe-modified form,” *Water Research*, Vol. 43, pp. 3659-3672 (2009).

[21] M. R. Adam *et al.*, “Current trends and future prospects of ammonia removal in wastewater: A comprehensive review on adsorptive membrane development,” *Separation and Purification Technology*, Vol. 213, pp.114-132 (2019).

[22] L. Gurreri, A. Tamburini, A. Cipollina, and G. Micale, “Electrodialysis applications in wastewater treatment for environmental protection and resources recovery: A systematic review on progress and perspectives,” *Membranes,* Vol. 10,pp. 146-148 (2020).

[23] F. N. Muya, C. E. Sunday, P. Baker, and E. Iwuoha, “Environmental remediation of

heavy metal ions from aqueous solution through hydrogel adsorption: A critical review," *Water Sci. Technol.*, Vol. 73, pp. 112-122 (2016).

[24] I. Heidmann and W. Calmano, "Removal of Zn(II), Cu(II), Ni(II), Ag(I) and Cr(VI) present in aqueous solutions by aluminium electrocoagulation," *Journal of Hazardous Materials*, Vol. 152, pp. 934-941 (2008).

[25] V. Van Tran, D. Park, and Y. C. Lee, "Hydrogel applications for adsorption of contaminants in water and wastewater treatment," *Environmental Science and Pollution Research*, Vol. 25, pp. 24569–24599 (2018).

[26] A. Bin Imran, T. Seki, and Y. Takeoka, "Recent advances in hydrogels in terms of fast stimuli responsiveness and superior mechanical performance," *Polymer Journal*, Vol. 42, pp. 839–851 (2010).

[27] L. W. Xia, R. Xie, X. J. Ju, W. Wang, Q. Chen, and L. Y. Chu, "Nano-structured smart hydrogels with rapid response and high elasticity," *Nat. Commun.*, Vol. 4 (2013).

[28] M. J. Ramazani-Harandi, M. J. Zohuriaan-Mehr, A. A. Yousefi, A. Ershad-Langroudi, and K. Kabiri, "Rheological determination of the swollen gel strength of superabsorbent polymer hydrogels," *Polym. Test.*, Vol. 25, pp. 470-474 (2006).

[29] Y. Li, G. Huang and X. Zhang, "Magnetic Hydrogels and Their Potential Biomedical Applications," *Advanced Functional Materials*, Vol. 23, pp. 660-672 (2013).

[30] H. Banerjee, M. Suhail, and H. Ren, "Hydrogel actuators and sensors for biomedical soft robots: Brief overview with impending challenges," *Biomimetics*, Vol. 3(3), pp. 15 (2018).

[31] E. M. Ahmed, "Hydrogel: Preparation, characterization, and applications: A review," *Journal of advanced research*, Vol. 6, pp. 105-121 (2015).

[32] W. Zhao, X. Jin and Y. Cong, "Degradable natural polymer hydrogels for articular cartilage tissue engineering," *Journal of Chemical Technology & Biotechnology*, Vol. 88, pp. 327-339, (2013)

[33] B.L. Carson et al, "Toxicology and biological Monitoring of Metals in Humans," *Lewia Publisher*, pp. 128-135 (1986).

[34] Hacker, M., Mikos, A., "Synthetic polymers, principles of regenerative medicine," *Elsevier*, 2nd ed., p. 587–622, (2011).

[35] N. Gulati, U. Nagaich, V. K. Sharma and R. L. Khosa, "Effect of Polymer and Cross Linking Agent on In Vitro Release of Quercetin from Microbeads," *Asian Journal of Pharmacy and Life Science*, Vol. 1(4), pp. 401-405 (2011).

[36] J. Zhu, “Bioactive modification of poly(ethylene glycol) hydrogels for tissue engineering,” *Biomaterials*, Vol. 31, pp. 4639-4656 (2010).

[37] A. Ramamurthi and I. Vesely, “Ultraviolet light-induced modification of crosslinked hyaluronan gels,” *Journal of Biomedical Materials Research*, Part A, Vol. 66A, pp. 317-329 (2003).

[38] B. K. Denizli, H. K. Can and Z. M. O. Rzaev, “Preparation conditions and swelling equilibria of dextran hydrogels prepared by some crosslinking agents,” *Polymer*, Vol. 45, pp. 6431-6435 (2004).

[39] N. Reddy, R. Reddy, & Q. Jiang, (2015). Crosslinking biopolymers for biomedical applications. *Trends in Biotechnology,* Vol.33, pp. 362–369 (2015).

[40] C. K. Kuo,and P. X. Ma, “Ionically crosslinked alginate hydrogels as scaffolds for tissue engineering: Part 1. Structure, gelation rate and mechanical properties,” *Biomaterials*, Vol. 22, pp. 511-521 (2001).

[41] T. Tanaka, “Collapse of Gels and the Critical Endpoint,” *Physical Review Letters*, Vol. 40, pp. 820-823 (1978).

[42] Y. Hirokawa and T. Tanaka, “Volume phase transition in a nonionic gel,” *The Journal of Chemical Physics*, Vol. 81, pp. 6379-6380 (1984).

[43] T. Amiya, Y. Hirokawa and Y. Hirose, “Reentrant phase transition of Nisopropylacrylamide gels in mixed solvents,” *The Journal of Chemical Physics*, Vol. 86, pp. 2375-2379 (1987).

[44] C. Alarcón, S. Pennadam, and C. Alexander, “Stimuli responsive polymers for biomedical applications,” *Chemical Society Reviews*, Vol. 34, pp. 276-285 (2005).

[45] T. Tanaka, I. Nishio and S.-T. Sun, “Collapse of Gels in an Electric Field,” *Science*, Vol. 218, pp. 467 (1982).

[46] Y. Osada, H. Okuzaki and H. Hori, “A polymer gel with electrically driven motility,” *Nature*, Vol. 355, pp. 242 (1992).

[47] T. Tanaka, D. Fillmore, S.-T. Sun et al., “Phase Transitions in Ionic Gels,” *Physical Review Letters*, Vol. 45, pp. 1636-1639 (1980).

[48] M. Irie, “Stimuli-responsive poly(N-isopropylacrylamide). Photo- and chemicalinduced phase transitions,” *Responsive Gels: Volume Transitions II*, Vol. 110, pp. 49-65 (1993).

[49] A. Suzuki and T. Tanaka, “Phase transition in polymer gels induced by visible light,” *Nature*, Vol. 346, pp. 345-347 (1990).

[50] D. Szabó, G. Szeghy and M. Zrinyi, “Shape Transition of Magnetic Field Sensitive Polymer Gels,” *Macromolecules,* Vol. 31, pp. 6541-6548 (1998).

[51] A. S. Hoffman, “Conventional and Environmentally-Sensitive Hydrogels for Medical and Industrial Uses: A Review Paper,” *Polymer gels,* pp. 289-290 (1991).

[52] C. d. l. H. Alarcón, S. Pennadam and C. Alexander, “Stimuli responsive polymers for biomedical applications,” *Chemical Society Reviews*, Vol. 34, pp. 276-285 (2005).

[53] B. Jeong, M. R. Kibbey and J. C. Birnbaum, “Thermogelling Biodegradable Polymers with Hydrophilic Backbones: PEG-g-PLGA,” *Macromolecules,* Vol. 33, pp. 8317-8322 (2000).

[54] L. Chen, Z. Tian and Y. Du, “Synthesis and pH sensitivity of carboxymethyl chitosan-based polyampholyte hydrogels for protein carrier matrices,” *Biomaterials*, Vol. 25, pp. 3725-3732 (2004).

[55] D. Schmaljohann, “Thermo- and pH-responsive polymers in drug delivery,” *Advanced Drug Delivery Reviews*, Vol. 58, pp. 1655-1670 (2006)

[56] H. G. Schild, “Poly(N-isopropylacrylamide): experiment, theory and application,” *Progress in Polymer Science*,” Vol. 17, pp. 163-249 (1992).

[57] M. Shibayama, T. Norisuye and S. Nomura, “Cross-link Density Dependence of Spatial Inhomogeneities and Dynamic Fluctuations of Poly(Nisopropylacrylamide) Gels,” *Macromolecules,* Vol. 29, pp. 8746-8750 (1996).

[58] I. Idziak, D. Avoce and D. Lessard, “Thermosensitivity of Aqueous Solutions of Poly(N,N-diethylacrylamide),” *Macromolecules*, Vol. 32, pp. 1260-1263 (1999).

[59] R. A. Horne, J. P. Almeida and A. F. Day, “Macromolecule hydration and the effect of solutes on the cloud point of aqueous solutions of polyvinyl methyl ether: A possible model for protein denaturation and temperature control in homeothermic animals,” *Journal of Colloid and Interface Science*, Vol. 35, pp. 7784 (1971).

[60] L. M. Mikheeva, N. V. Grinberg and A. Y. Mashkevich, “Microcalorimetric Study of Thermal Cooperative Transitions in Poly(N-vinylcaprolactam) Hydrogels,” *Macromolecules,* Vol. 30, pp. 2693-2699 (1997).

[61] K. Van Durme, S. Verbrugghe and F. E. Du Prez, “Influence of Poly(ethylene oxide) Grafts on Kinetics of LCST Behavior in Aqueous Poly(Nvinylcaprolactam) Solutions and Networks Studied by Modulated Temperature DSC,” *Macromolecules,* Vol. 37, pp. 1054-1061 (2004).

[62] E. E. Makhaeva, H. Tenhu and A. R. Khokhlov, “Conformational Changes of

Poly(vinylcaprolactam) Macromolecules and Their Complexes with Ionic Surfactants in Aqueous Solution," *Macromolecules*, Vol. 31, pp. 6112-6118 (1998).

[63] T. Aoki, M. Kawashima and H. Katono et al., "Temperature-Responsive Interpenetrating Polymer Networks Constructed with Poly(acrylic acid) and Poly(N,N-dimethylacrylamide)," *Macromolecules*, Vol. 27, pp. 947-952 (1994).

[64] J. Thévenot, H. Oliveira, O. Sandre et al., "Magnetic responsive polymer composite materials," *Chemical Society Reviews*, Vol. 42, pp. 7099-7116 (2013).

[65] T. Hoare, J. Santamaria and G. F. Goya, "A Magnetically Triggered Composite Membrane for On-Demand Drug Delivery," *Nano Letters*, Vol. 9, pp. 3651-3657 (2009).

[66] T. Hoare, B. P. Timko and J. Santamaria, "Magnetically Triggered Nanocomposite Membranes: A Versatile Platform for Triggered Drug Release," *Nano Letters*, Vol. 11, pp. 1395-1400 (2011).

[67] B. P. Timko, T. Dvir and D. S. Kohane, "Remotely Triggerable Drug Delivery Systems," *Advanced Materials*, Vol. 22, pp. 4925-4943 (2010).

[68] H. H. Himstedt, Q. Yang and L. P. Dasi, "Magnetically Activated Micromixers for Separation Membranes," *Langmuir*, Vol. 27, pp. 5574-5581 (2011).

[69] Q. Yang, H. H. Himstedt and M. Ulbricht, "Designing magnetic field responsive nanofiltration membranes," *Journal of Membrane Science*, Vol. 430, pp. 70-78 (2013).

[70] A. Y. Gebreyohannes, R. Mazzei and M. Y. Marei Abdelrahim, "Phosphotriesterase-Magnetic Nanoparticle Bioconjugates with Improved Enzyme Activity in a Biocatalytic Membrane Reactor," *Bioconjugate Chemistry*, Vol. 29, pp. 2001-2008 (2018).

[71] Himstedt, H. H., Yang, Q., Dasi, L. P., Qian, X. H., Wickramasinghe, S. R. and Ulbricht, M., "Magnetically Activated Micromixers for Separation Membranes," *Langmuir*, Vol. 27, pp. 5574-5581, 2011.

[72] S. J. Grainger and M. E. H. El-Sayed, "Stimuli-sensitive particles for drug delivery," *Biologically-Responsive Hybrid Biomaterials*, pp. 171-190 (2010).

[73] G. R. Newkome, G. R. Baker, S. Arai, M. J. Saunders, P. S. Russo, K. J. Theriot, C. N. Moorefield, L. E. Rogers, J. E. Miller, T. R. Lieux, M. E. Murray, B. Phillips and L. Pascal, "Cascade molecules. Part 6. Synthesis and characterization of twodirectional cascade molecules and formation of aqueous gels," *Journal of American Chemical Society*, Vol. 112, pp.8458–8465 (1990).

[74] G. S. Kumar and D. C. Neckers, “Photochemistry of azobenzene-containing polymers,” *Chemical Reviews,* Vol. 89, pp. 1915-1925 (1989).

[75] J. Szejtli, “Introduction and General Overview of Cyclodextrin Chemistry,” *Chemical Reviews,* Vol. 98, pp. 1743-1754 (1998).

[76] D. T. Simon, S. Kurup and K. C. Larsson, “Organic electronics for precise delivery of neurotransmitters to modulate mammalian sensory function,” *Nature Materials,* Vol. 8, pp. 742, (2009).

[77] P. M. George, D. A. LaVan and J. A. Burdick, “Electrically Controlled Drug Delivery from Biotin-Doped Conductive Polypyrrole,” *Advanced Materials*, Vol. 18, pp. 577-581 (2006).

[78] D. Svirskis, J. Travas-Sejdic and A. Rodgers, “Electrochemically controlled drug delivery based on intrinsically conducting polymers,” *Journal of Controlled Release*, Vol. 146, pp. 6-15 (2010).

[79] H. Ringsdorf, J. Venzmer and F. M. Winnik, “Interaction of HydrophobicallyModified Poly-N-isopropylacrylamides with Model Membranes or Playing a Molecular Accordion,” *Angewandte Chemie International Edition in English*, Vol. 30, no. 3, pp. 315-318 (1991)

[80] J. K. Carrow and A. K. Gaharwar, "Bioinspired Polymeric Nanocomposites for Regenerative Medicine," *Macromol. Chem. Physic*., vol. 216, pp. 248-264 (2015).

[81] I. Maity, D. B. Rasale, and A. K. Das, "Sonication induced peptide-appended bolaamphiphile hydrogels for in situ generation and catalytic activity of Pt nanoparticles," *Soft Matter*, vol. 8, pp. 5301-5308 (2012).

[82] R. Fuhrer, E. K. Athanassiou, N. A. Luechinger, and W. J. Stark, "Crosslinking Metal Nanoparticles into the Polymer Backbone of Hydrogels Enables Preparation of Soft, Magnetic Field-Driven Actuators with Muscle-Like Flexibility," *Small*, vol. 5, pp. 383-388 (2009).

[83] S. Cometa, R. Iatta, M. A. Ricci, C. Ferretti, and E. De Giglio, "Analytical characterization and antimicrobial properties of novel copper nanoparticle–loaded electrosynthesized hydrogel coatings," *J Bioact. Compat. Pol.*, vol. 28, pp. 508-522 (2013).

[84] S. R. Shirsath, A. P. Hage, M. Zhou, S. H. Sonawane, and M. Ashokkumar, "Ultrasound assisted preparation of nanoclay Bentonite-FeCo nanocomposite hybrid hydrogel: A potential responsive sorbent for removal of organic pollutant from water,"

Desalination, vol. 281, pp. 429-437 (2011).

[85] A. L. Daniel-da-Silva, R. S. Carvalho, and T. Trindade, "Magnetic Hydrogel Nanocomposites and Composite Nanoparticles; a Review of Recent Patented Works," *Recenr Pat. Nanotech*., vol. 7, pp. 153-166 (2013).

[86] O. Ozay, S. Ekici, Y. Baran, N. Aktas, and N. Sahiner, "Removal of toxic metal ions with magnetic hydrogels," *Water Res*., vol. 43, pp. 4403-4411 (2009).

[87] G. S. Alvarez, C. Hélary, A. M. Mebert, X. Wang, T. Coradin, and M. F. Desimone, "Antibiotic-loaded silica nanoparticle–collagen composite hydrogels with prolonged antimicrobial activity for wound infection prevention," *J. Mater. Chem. B*, vol. 2, pp. 4660-4670 (2014).

[88] S. K. Samanta, A. Pal, S. Bhattacharya, and C. N. R. Rao, "Carbon nanotube reinforced supramolecular gels with electrically conducting, viscoelastic and nearinfrared sensitive properties," *J. Mater. Chem*., vol. 20, pp. 6881-6890 (2010).

[89] C.-W. Lo, D. Zhu, and H. Jiang, "An infrared-light responsive graphene-oxide incorporated poly(N-isopropylacrylamide) hydrogel nanocomposite," *Soft Matter*, vol. 7, pp. 5604-5609 (2011).

[90] C. Ninh, M. Cramer, and C. J. Bettinger, "Photoresponsive hydrogel networks using melanin nanoparticle photothermal sensitizers," *Biomater Sci*., vol. 2, pp. 766-774 (2014).

[91] A. O. Moughton, M. A. Hillmyer, and T. P. Lodge, "Multicompartment Block Polymer Micelles," *Macromolecules*, vol. 45, pp. 2-19 (2012).

[92] R. T. Chacko, J. Ventura, J. Zhuang, and S. Thayumanavan, "Polymer nanogels: A versatile nanoscopic drug delivery platform," *Adv. Drug Delivery Rev*., vol. 64, pp. 836-851 (2012).

[93] G. L. Li, H. Möhwald, and D. G. Shchukin, "Precipitation polymerization for fabrication of complex core–shell hybrid particles and hollow structures," *Chem. Soc. Rev*., vol. 42, pp. 3628-3646 (2013).

[94] A. D. Schlüter, A. Halperin, M. Kröger, D. Vlassopoulos, G. Wegner, and B. Zhang, "Dendronized Polymers: Molecular Objects between Conventional Linear Polymers and Colloidal Particles," *ACS Macro Lett*., vol. 3, pp. 991-998 (2014).

[95] Y. Wu, Z. Zhou, Q. Fan, L. Chen, and M. Zhu, "Facile in-situ fabrication of novel organic nanoparticle hydrogels with excellent mechanical properties," *J. Mater. Chem*., vol. 19, pp. 7340-7346 (2009).

[96] O. V. Salata, "Applications of nanoparticles in biology and medicine," *Journal of Nanobiotechnology*, vol. 2, pp. 3 (2004).

[97] J. P. Wolfgang, G. Daniele, P. Teresa, Z. Daniela, M. Christine, C. W. Shara., "Biological applications of colloidal nanocrystals," *Nanotechnology*, vol. 14, pp. R15 (2003).

[98] R. Wang et al., “Biogenic manganese oxides generated by green algae Desmodesmus sp. WR1 to improve bisphenol A removal,” *J. Hazard. Mater*., Vol. 339, pp. 310-319 (2017).

[99] I. O. Sosa, C. Noguez, and R. G. Barrera, “Optical properties of metal nanoparticles with arbitrary shapes,” *J. Phys. Chem. B*, Vol. 107, pp. 6269-6275 (2003).

[100] A. K. Gupta and M. Gupta, “Synthesis and surface engineering of iron oxide nanoparticles for biomedical applications,” *Biomaterials*. Vol. 26, pp. 3995-4021 (2005).

[101] J. R. J. Delben *et al.*, “Synthesis and thermal properties of nanoparticles of bioactive glasses containing silver,” *J. Therm. Anal. Calorim.*, Vol. 97, pp. 433–436 (2009).

[102] A. D. Jenkins, R. F. T. Stepto, P. Kratochvíl, and U. W. Suter, “Glossary of basic terms in polymer science (IUPAC Recommendations 1996),” *Pure Appl. Chem.*, Vol. 68(12), pp. 2287-2311, (1996).

[103] S. Kobayashi and A. Makino, “Enzymatic polymer synthesis: an opportunity for green polymer chemistry,” *Chem. Rev.*, Vol. 109(11), pp. 5288–5353 (2009)

[104] A. M. Muzafarov *et al.*, “Macromolecular nano-objects as a promising direction of polymer chemistry,” in *Polymer Science - Series C*, 2011. yakushev, M.A. Obrezkova, I.B. Meshkov, N.V. Voronina, O.V. Novozhilov, Vol. 53(7), pp. 1217–1230 (2011).

[105] M. A. Tasdelen, M. U. Kahveci, and Y. Yagci, “Telechelic polymers by living and controlled/living polymerization methods,” *Progress in Polymer Science (Oxford)*, Vol. 36(4), pp. 455–567 (2011).

[106] B. Brooks, “Suspension polymerization processes,” *Chemical Engineering and Technology*, Vol. 31(2), pp. 215–299 (2010).

[107] E. Vivaldo-Lima, P. E. Wood, A. E. Hamielec, and A. Penlidis, “An Updated Review on Suspension Polymerization,” *Ind. Eng. Chem. Res.*, Vol. 36(4), pp. 939-965 (1997).

[108] M. Okubo, Y. Konishi, and H. Minami, “Production of hollow polymer particles by suspension polymerization,” *Colloid Polym. Sci.*, Vol. 276(7), pp. 638—642 (1998).

[109] A. N. Mujumdar, S. G. Young, R. L. Merker, and J. H. Magill, “A Study of Solution

Polymerization of Polyphosphazenes," *Macromolecules*, Vol. 23(1), pp. 14-21 (1990).

[110] K. J. Abbey, "Polymerization Kinetics by Precision Densimetry" *Emulsion Polymers and Emulsion Polymerization*, Vol. 165, pp. 345-356, (1980).

[111] A. H. Abdel-Alim and A. E. Hamielec, "Bulk polymerization of vinyl chloride," *J. Appl. Polym. Sci.*, Vol. 16, pp. 783-799 (1972).

[112] D. K. Adebekun and F. J. Schork, "Continuous Solution Polymerization Reactor Control. 2. Estimation and Nonlinear Reference Control during Methyl Methacrylate Polymerization," *Ind. Eng. Chem. Res.*, Vol. 28(12), pp. 1846-1861 (1989).

[113] G. Arzamendi, J. R. Leiza, and J. M. Asua, "Semicontinuous emulsion copolymerization of methyl methacrylate and ethyl acrylate," *J. Polym. Sci. Part A Polym. Chem.*, Vol. 29(11), pp. 1549-1559 (1991).

[114] M. J. Ballard, D. H. Napper, and R. G. Gilbert, "Theory of emulsion copolymerization kinetics," *J. Polym. Sci. A1.*, Vol. 19, pp. 939-954 (1981).

[115] Nortona, L. W., Tegnella, E., Toporekb, S. S., and Reicherta, W. M., "In vitro characterization of vascular endothelial growth factor and dexamethasone releasing hydrogels for implantable probe coatings" *Biomaterials*, vol. 26, pp. 3285–3297 (2005).

[116] M Peng, H. Wang, Y. Chen. "Encapsulation of microgels with polystyrene (PS): A novel method for the preparation of hollow PS particles", *Materials Letters*, Vol 62, pp. 1535–1538 (2008).

[117] M. Devine, M. Juba, P. Russo, and B. Bishop, "Structurally stable N- t -butylacrylamide hydrogel particles for the capture of peptides", *Colloids and Surfaces B: Biointerfaces*, Vol. 161, pp. 471–479 (2018).

[118] Yan, X., Li, J., and Möhwald, H., "Templating Assembly of Multifunctional Hybrid Colloidal Spheres" *Advanced Materials*, vol. 24, pp. 2663-2667, 2012.

[119] Bhattacharya, S., Eckert, F., Boyko, V., and Pich, A., "Temperature-, pH-, and Magnetic-Field-Sensitive Hybrid Microgels" *Small*, vol. 3, pp. 650-657, 2007.

[120] J. I. Kim, C. J. Chun, B. Kim, J. M. Hong, J. Cho, S. H. Lee, S. Song, "Thermosensitive/magnetic poly(organophosphazene) hydrogel as a long-term magnetic resonance contrast platform", *Biomaterials*, Vol. 33, pp. 218–224 (2012).

[121] Aragay, G., Porns, J., and Merkochi, A., "Recent trends in macro-, micro-, and nanomaterial- based tools and strategies for heavy-metal detection," *Chem. Rev.*, vol. 111, pp. 3433-3458, 2011.

[122] Nagh, W. S. W., and Hanafiah M. K. A. M., “Removal of heavy metal ions from wastewater by chemically modified plant wastes as adsorbents,” *Bio. Tech.*, vol. 99, pp. 3935-3948, 2008.

[123] Charerntanyarak, L., “Heavy metals removal by chemical coagulation and precipitation,” *Wa. Sci. Technol.*, vol. 39, pp. 135-138, 1999.

[124] Dabrowski, A., Hubicki, Z., Podkoscielny, P., and Robens, E., “Selective removal of the heavy metal ions from waters and industrial wastewater by ion exchange method,” *Chemosphere*, vol. 56, pp. 91-106, 2004.

CHAPTER 2
Experimental

2.1 Materials and instruments

2.1.1 Chemicals and reagents

The chemicals and reagents used in this research were analytical grade and used without further purification. Distilled water was used as a solvent to prepare most of the solutions of this work. The chemicals and reagents which were used in this research are given below:

1. *N*-isopropylacrylamide (NIPAm)
   (KJ Chemicals Corporation, Japan)
2. 2-Acrylamido-2-methylpropane sulfonic acid (AMPS)
   (Sigma Aldrich, Germany)
3. Acrylic Acid (AAc)
   (LOBA Chemie, India)
4. *N*,*N*-methylenebisacrylamide (BIS)
   (Across organics, United States)
5. Potassium persulfate (KPS)
   (Sigma Aldrich, United States)
6. Tetramethylethylenediamine (TEMED)
   (Sigma Aldrich, United States)
7. Sodium dodecyl sulfate (SDS)
   (Sigma Aldrich,Germany)
8. Mercuric chloride ($HgCl_2$)
   (Sigma Aldrich, Germany)
9. Iron trichloride ($FeCl_3$)
   (Sigma Aldrich, Germany)
10. Iron dichloride ($FeCl_2$)
    (Sigma Aldrich, Germany)
11. Sodium Hydroxide (NaOH)
    (EMPROVE, Germany)
12. Nickel chloride hexahydrate ($NiCl_2$.6H2O)
    (Sigma Aldrich, Germany)
13. Sodium dodecyl sulfate (SDS)
    (Sigma Aldrich, Germany)
14. Dopamine hydrochloride ($C_8H_{11}NO_2$)

(Sigma Aldrich, Germany)

2.1.2 Instruments

Analysis of the samples was performed using the following instruments:

- Field emission scanning electron microscopy (JSM-7600F, Tokyo, Japan)
- UV-visible Spectrophotometer (Shimadzu-1800)
- Digital Balance (AB 265/S/SACT METTLER, Toledo, Switzerland)
- Dynamic light scattering (DLS; Zetasizer Nano ZS 90; Malvern, UK)
- Freeze dryer (Heto FD3)
- Oven (Lab Tech, LDO-030E)
- Shaker machine (Stuart, orbital shaker, SSL1)
- pH meter (Hanna, HI 8424, Romania)

2.2 Method of preparation

2.2.1 Fabrication of Fe_3O_4 nanocrystal

An iron salt solution was obtained by mixing 0.005mol $FeCl_3$ and 0.0025mol $FeCl_2$ in 50ml deoxygenated distilled water. 20 milliliters of 1.5M NaOH was rapidly poured into the salt solution under magnetic stirring at room temperature. A black precipitate instantly formed. After continuously stirring for 10min, the precipitate was separated by centrifugation and washed with the deoxygenated distilled water four times, followed with the deoxygenated anhydrous ethanol once, then vacuum-dried at 50 ^{o}C overnight, and Fe_3O_4 nanocrystals were obtained [1-3]. The size and morphology of Fe_3O_4 particles were observed by a scanning electron microscope (SEM).

2.2.2 Fabrication of Fe_3O_4-PD nanocrystal

To coat Fe_3O_4 cores with the polydopamine (PD) shell, 80 mg of Fe_3O_4 and 80 mg of dopamine hydrochloride were dissolved in 40 mL of Tris buffer solution (10 mM, pH = 8.5). After shaking for 24 h at room temperature, the products were separated and washed with ultrapure water and ethanol several times [4-6].

2.2.3 Fabrication of Ni nanocrystal

First, 3.213 g of $NiCl_2.6H2O$ (1.35 mol of $NiCl_2$) was dissolved in 3.75 g of distilled water. 2.822 g of 80% $N_2H_4.H2O$ (4.5 mol of N_2H_4) was poured into the solution instantaneously with vigorous stirring, which resulted in a pale violet precipitate. The precipitate on the wall was washed with additional distilled water (.50 ml) for ~60 s. The solution temperature increased up to ~65 ^{o}C by the exothermic formation of a Ni complex between $NiCl_2$ and N_2H_4. When the solution temperature became 50 ^{o}C by cooling in an ambient atmosphere, 2.88 g of a 50 wt% NaOH solution (3.6 mol of NaOH, the temperature of NaOH solution=20 ^{o}C) was poured instantaneously into the stock solution. The solution temperature initially decreased and then increased spontaneously up to the second maximum (~54 ^{o}C), after which it decreased again to room temperature. The reaction was complete 1 h after the temperature reached the second maximum (54 ^{o}C). The black Ni precipitate was washed six times with distilled water and dried at room temperature for 16 h under constant ventilation. For all the experimental conditions, approximately 100% of the Ni source solution was successfully converted into Ni particles [7-9]. The size and morphology of Ni particles were observed by a scanning electron microscope (SEM)

2.2.4 Fabrication of Ni-PD nanocrystal

To coat the surface of Ni nanoparticles with polydopamine, dopamine hydrochloride (0.05 g) and the prepared Ni nanoparticles (0.15 g) were dispersed in 70 mL of Tris buffer (pH = 8.5). The mixture was stirred at 60 ^{o}C for 24 hours. The prepared polydopamine coated Ni nanoparticles (Ni–PD) were washed with distilled water thoroughly [10-11].

2.2.5 Fabrication of submicrometer-sized hydrogels

Four types of hydrogel were fabricated i.e. (i) N-isopropylacrylamide-co- Acrylic acid hydrogel (NIPAm-co-AAc) (ii) *N*-isopropylacrylamide-co- 2Acrylamido-2-methylpropane sulfonic acid hydrogel (NIPAm-co-AMPS) (iii) Iron oxide-poly dopamine-N-isopropylacrylamide-co- 2Acrylamido-2-methylpropane sulfonic acid hydrogel (Fe_3O_4-PD-NIPAm-co-AMPS) hydrogel (iv) Nickel-poly dopamine-*N*-isopropylacrylamide-co-2Acrylamido-2-methylpropane sulfonic acid hydrogel (Ni-PD-NIPAm-co-AMPS) hydrogel. To fabricate these hydrogels BIS as a cross-linker, KPS as an initiator, TEMED as an accelerator, SDS as a surfactant and deionized water as a solvent were used. The recipe for hydrogels with different nanoparticles with other gel precursors (e.g. cross-linker, initiator and solvent) are appended in the following table.

Table-1: Recipe of gel precursors to synthesize NIPAm-co-AAc, NIPAm-co-AMPS, Fe_3O_4-PD-NIPAm-co-AMPS and Ni-PD-NIPAm-co-AMPS hydrogel particle

Type	**NIPAm (mM)**	**AMPS (mM)**	**KPS (mM)**	**BIS (mM)**	**TEMED (ml)**	**NP (Fe_3O_4-PD/ Ni-PD) (g)**	**SDS (mM)**	**Distilled water (ml)**
NIPAm-co-AAc	38.4	.15	0.614	0.428	0	0	0.368	260
NIPAm-co-AMPS	38.4	1	0.614	0.428	0.04	0	0.368	260
Fe_3O_4-PD-NIPAm-co-AMPS	38.4	1	0.614	0.428	.04	0.0350 g Fe_3O_4-PD	0.368	260
Ni-PD-NIPAm-co-AMPS	38.4	1	0.614	0.428	.04	0.0350 g Ni-PD	0.368	260

2.2.6 Preparation of submicrometer-sized gel particles

At first, two types of submicrometer-sized thermos-responsive hydrogel particles were prepared where NIPAm was used as the main monomer and AAc and AMPS were used as comonomers. To fabricate NIPAm-co-AAc BIS and KPS were use as cross-linker and initiator, respectively. SDS was used as a surfactant. NIPAm (38.4 mmol), AAc (.15mmol), BIS

(0.428mmol), SDS (0.368 mmol) were dissolved in the distilled water. The pre-gel solution was kept at 70 °C under a stream of nitrogen for one hour to make the solution free from oxygen. Following the addition of KPS (0.614 mmol), the polymerization was carried out at 70 °C for 4.5 h under a nitrogen atmosphere. The micro and nano gel were purified by dialysis for > 7 days in distilled water.

The NIPAm -co-AMPS was prepared by following the same procedure as NIPAm-co-AMPS. But emulsion polymerization is difficult in the presence of ionic moiety. To accelerate the reaction 0.04 ml TEMED were dissolved in the mixture.

To fabricate our desired thermo and magnetic responsive submicrometer-sized hydrogels particles Fe_3O_4-PD-NIPAm-co-AMPS and Ni-PD-NIPAm-co-AMPS, NIPAm was used as the main monomer, AMPS was used as comonomer. In this polymerization, BIS and KPS were used as cross-linker and initiator, respectively. To accelerate the reaction TEMED was used as an accelerator, and SDS was used as a surfactant. Fe_3O_4-PD and Ni-PD magnetic nanocomposites were used to develop the magnetic property of hydrogel.

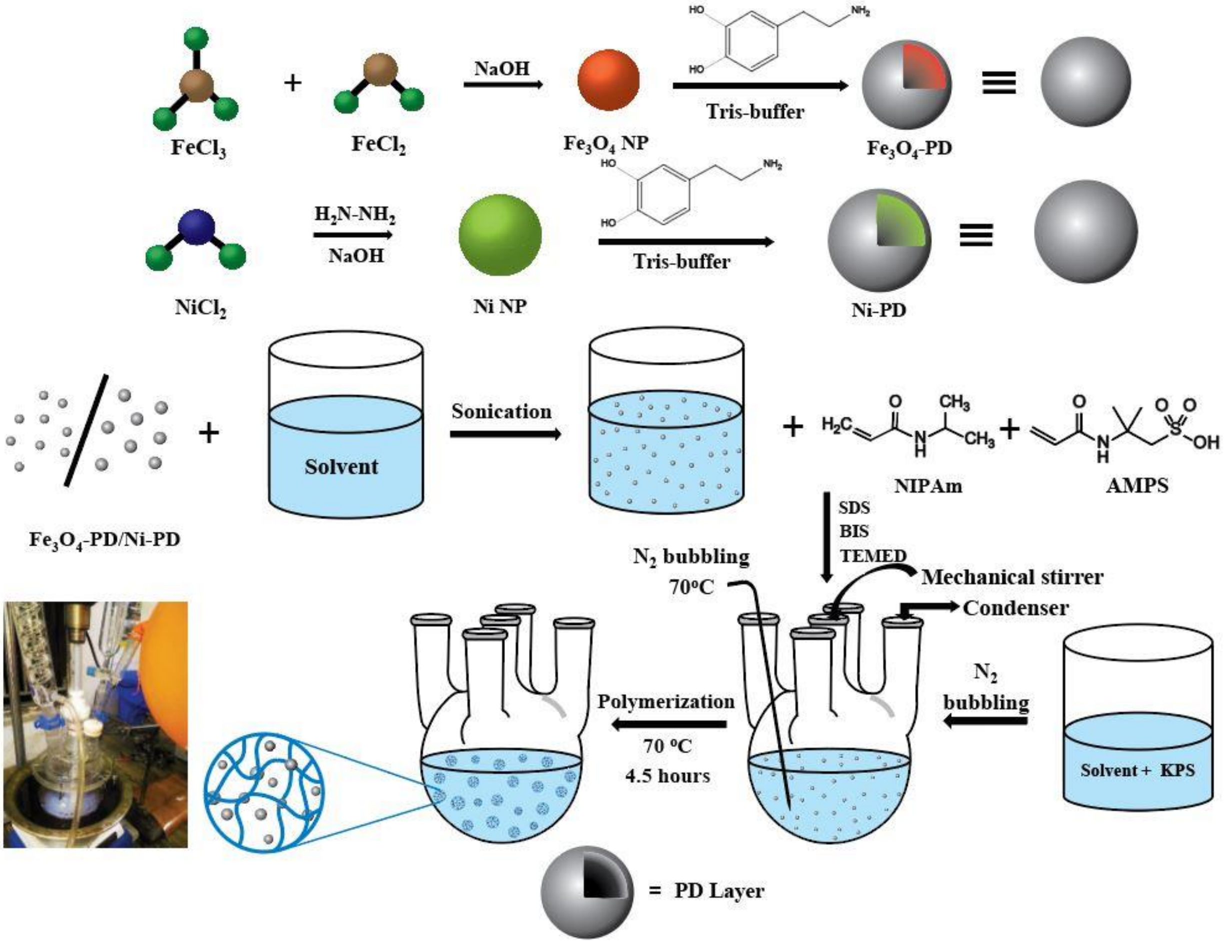

Figure 2.2.1 Synthesis scheme of hydrogel

First, 0.0350 g Fe_3O_4-PD (or 0.0350 g Ni-PD) was dispersed in 240 ml distilled water by sonication. NIPAm (38.4 mmol), AMPS (1mmol), BIS (0.428mmol), SDS (0.368 mmol) and 0.04 ml TEMED were dissolved in the distilled water The pre-gel solution was kept at 70 °C under a stream of nitrogen for one hour to make the solution free from oxygen. Following the addition of KPS (0.614 mmol), the polymerization was carried out at 70 °C for 4.5 h under a nitrogen atmosphere. The micro and nano gel were purified by dialysis for > 7 days in distilled water [12].

2.2.7 Dialysis

150 Himedia dialysis membrane was used which average flat width 37.70 mm, average diameter 25.4 mm, capacity approx. 5.07 ml/cm. To prepare the dialysis membrane was washed with running water for 3-4 hours. Then it was washed with 0.3% solution (80 °C) of Sodium Sulfide for one minute and then washed again with 60 °C hot water for two minutes. After that, it was washed with a 0.2% (v/v) solution of Sulfuric acid. Finally, the dialysis tube was rinsed with hot water [13].

2.3 Sample characterization

2.3.1 FTIR analysis of nanoparticles

FT-IR analysis of hydrogels was studied in FT-IR spectrometer in the region of 4000-1000 cm^{-1}. Small amount of sample was then oven-dried at 50°C and collected into a vial. A pellet was made for FT-IR analysis with the sample. Then samples were mixed and ground well with KBr crystal into mortar by using a pestle. Using 8-10 tons pressure a sample pellet was made by a manual metallic pellet maker and carefully placed in the path of IR beam for analysis [14].

2.3.2 Field emission-scanning electron microscopy (FE-SEM):

The surface morphology of the magnetic nanoparticles and dopamine coated magnetic nanoparticles were analyzed using Field emission-scanning electron microscopy (FE-SEM). The completely air-dried samples were glued on a conducting carbon strip. The sample-loaded strip was then mounted to a chamber evacuated to ~ 10^{-3} to 10^{-4} tor. A very thin platinum layer (a few nanometers thick) was incorporated by sputtering platinum on the sample to ensure the conductivity of the sample surface. The sample was then placed in the sample chamber to view its surface. The microscope was operated at an accelerating voltage of 5.0 kV.

2.3.3 Dynamic light scattering (DLS)

The hydrodynamic diameters of the submicrometer-sized hydrogels were determined by dynamic light scattering (DLS; Zetasizer Nano ZS 90; Malvern, UK). The scattering angle was kept at 90° and the wavelength was set at 632.8 nm (He-Ne laser beam).

2.4 Heavy metal removal analysis

2.4.1 Hg^{2+}removal analysis:

1.5 mL (~4mg) hydrogel dispersion was immersed in 20 ml of 60 ppm $HgCl_2$ solution and shaken at 100 rpm for 24 hours. DPC was used for spectrophotometric determination of Hg (II). DPC solution was prepared by dissolving 250 mg of DPC in 50mL methanol. After 4 h, $HgCl_2$ and DPC solution were mixed. Spectrophotometric measurements were executed using a Shimadzu 160A Ultraviolet-Visible spectrophotometer at room temperature. Distilled water was chosen as the reference. The equilibrium concentrations of Hg^{2+} solutions were determined using the calibration curve.

2.4.2 Cr^{6+}removal analysis:

1.5 ml (~4mg) hydrogel was immersed in 20 ml of 10 ppm potassium dichromate solution at room temperature and shaken at 100 rpm for 24 hours. DPC was used for the spectrophotometric determination of Cr (VI). DPC solution was prepared by dissolving 250mg of DPC in 50mL methanol. After 4 h, potassium dichromate and DPC solution were mixed. Spectrophotometric measurements were executed using a Shimadzu 1800 a UV-Visible spectrophotometer at room temperature. Distilled water was chosen as the reference. The equilibrium concentrations of Cr^{6+} solutions were determined using a calibration curve. [15].

Reference:

[1] Y. P. He, S. Q. Wang, C. R. Li, Y. M. Miao, Z. Y. Wu, and B. S. Zou, “Synthesis and characterization of functionalized silica-coated Fe_3O_4 superparamagnetic nanocrystals for biological applications,” *J. Phys. D. Appl. Phys.*, Vol. 38, pp. 1342-1350 (2005).

[2] S. Rani, G.D. Varma, “Superparamagnetism and metamagnetic transition in Fe_3O_4 nanoparticles synthesized via co-precipitation method at different pH”, *Physica B: Condensed Matter*, Vol. 472, pp. 66–77 (2015).

[3] R. Valenzuela, M. C. Fuentes, C. Parra; J. Baeza, N. Duran, S.K. Sharma, M. Knobel, J. Freer, “Influence of stirring velocity on the synthesis of magnetite nanoparticles (Fe_3O_4) by the co-precipitation method”, *Journal of Alloys and Compounds*, Vol. 488, pp. 227–231 (2009).

[4] P. An, F. Zuo, Y.P. Wu, J. H. Zhang, Z. H. Zheng, X. B. Ding, Y. X. Peng, “Fast synthesis of dopamine-coated Fe_3O_4 nanoparticles through ligand-exchange method”, *Chinese Chemical Letters*, Vol. 23, pp. 1099–1102 (2012).

[5] Y. Xie *et al.*, “Highly regenerable mussel-inspired Fe_3O_4 @Polydopamine-Ag core-shell microspheres as catalyst and adsorbent for methylene blue removal,” *ACS Appl. Mater. Interfaces*, Vol. 6, pp. 8845–8852 (2014).

[6] N. Kemikli, H. Kavas, S. Kazan, A. Baykal, R. Ozturk. “Synthesis of protoporphyrin coated superparamagnetic iron oxide nanoparticles via dopamine anchor”, *Journal of Alloys and Compounds*, Vol. 502, pp. 439–444 (2010).

[7] J. Y. Choi *et al.*, “A chemical route to large-scale preparation of spherical and monodisperse Ni powders,” *J. Am. Ceram. Soc.*, Vol. 8, pp. 3020-3023 (2005).

[8] Y. Hou, H. Kondoh, T. Ohta, S. Gao, “Size-controlled synthesis of nickel nanoparticles”, Vol. *Applied Surface Science*, 241, pp. 218–222 (2005).

[9] N. Sahiner, H. Ozay, O. Ozay, N. Aktas, “New catalytic route: Hydrogels as templates and reactors for in situ Ni nanoparticle synthesis and usage in the reduction of 2- and 4-nitrophenols”, *Applied Catalysis A: General*, Vol. 385, pp. 201–207 (2010).

[10] F. Mahnaz, M. Mostafa-Al-Momin, M. Rubel, M. Ferdous, and M. S. Azam, “Mussel-inspired immobilization of Au on bare and graphene-wrapped Ni nanoparticles toward highly efficient and easily recyclable catalysts,” *RSC Adv.*, Vol. 9, pp. 30358-30369 (2019).

[11] C. Li, Y. Huang, J. Chen, “Dopamine-assisted one-pot synthesis of graphene@Ni@C composites and their enhanced microwave absorption performance”, *Materials Letters*, Vol. 154, pp. 136–139 (2015).

[12] J. D. Debord, S. Eustis, S. Byul Debord, M. T. Lofye, and L. A. Lyon, “Color-tunable colloidal crystals from soft hydrogel nanoparticles,” *Adv. Mater.*, Vol. 14, pp. 658-662 (2002).

[13] C. Ronco and S. Bowry, “Nanoscale modulation of the pore dimensions, size distribution and structure of a new polysulfone-based high-flux dialysis membrane,” *Int. J. Artif. Organs*, Vol. 24, pp. 726-735 (2001)

[14] K. Varaprasad, N. N. Reddy, S. Ravindra, K. Vimala, and K. M. Raju, “Synthesis and characterizations of macroporous poly(acrylamide-2- acrylamido-2-methyl-1-propanesulfonic acid) hydrogels for in vitro drug release of ranitidine hydrochloride,” *Int. J. Polym. Mater. Polym. Biomater.*, Vol. 60, pp. 490-503 (2011).

[15] P. Yuan *et al.*, “Removal of hexavalent chromium [Cr(VI)] from aqueous solutions by the diatomite-supported/unsupported magnetite nanoparticles,” *J. Hazard. Mater.*, Vol. 173, pp. 614–621 (2010)

CHAPTER 3
Results and Discussion

3.1 Synthesis of Hydrogel:

Different types of polymerization processes are generally used for hydrogel synthesis. The free-radical polymerization process is one of the most common and facile polymerization processes for hydrogel synthesis. Three fundamental steps of free radical polymerization are initiation, propagation, and termination. In the initiation step, the initiator produces free radicals. Chemical initiation, photochemical initiation, thermal initiation, radiation initiation are the typical initiation process. Thus, the process of chain initiation involves two steps, the first being the decomposition of the initiator (e.g. KPS, APS or AIBN) to yield a pair of free radicals R·, and the second the addition of a monomer to the primary radical R· to yield the chain radical, which is called the initiation. Following its generation, the free radical then reacts with a vinyl monomer; that is, it adds to one of the electrons of the double bond of the vinyl monomer and the remaining electron becomes the new free radical.

$$I \longrightarrow 2\,R^{\cdot}$$

$$R^{\cdot}+M \longrightarrow RM^{\cdot}$$

Figure 3.1.1 Schematic illustration of the Initiation step

The propagation step would theoretically continue until all monomers are consumed. However, pairs of radicals also tend to react with each other and thus annihilate their activities. Combination or disproportionation are the two ways of termination. In the case of combination or coupling, two growing polymer chains react to forming a single nonreactive polymer chain.

$$RM_1^{\cdot}+M \longrightarrow RM_2^{\cdot}$$

$$RM_3^{\cdot}+M \longrightarrow RM_4^{\cdot}$$

$$RM_2^{\cdot}+M \longrightarrow RM_3^{\cdot}$$

$$RM_x^{\cdot}+M \longrightarrow RM_{x+1}^{\cdot} \quad \ldots\ldots\ldots \quad \ldots.$$

Figure 3.1.2 Schematic illustration of the Propagation step

And in case of disproportionation, a hydrogen atom is transferred from one radical to the other resulting in two polymers, one with a saturated end and the other with an unsaturated end and each with an initiator fragment. Usually, there is no need to distinguish between these two different types of termination reactions.

(a) $M_x^{\cdot} + M_y^{\cdot} \longrightarrow M_{x+y}$

(b) $M_x^{\cdot} + M_y^{\cdot} \longrightarrow M_x + M_y$

Figure 3.1.3 Schematic illustration of theTermination (a) Combination (b) Disproportionation

In this work, the free radical precipitation polymerization process has been employed. NIPAm-based hydrogels are prepared mainly by free-radical crosslinking copolymerization of the AMPS monomer with KPS as an initiator, TEMED as an accelerator, SDS as a surfactant and BIS as a cross-linker were used.

To develop the magnetic properties of submicrometer-sized hydrogel Fe_3O_4 and Ni nano particles were used. Chemical coprecipitation method was used to prepare the magnetite Fe_3O_4 nano particles. Two types of Fe salt were used, $FeCl_2$ and $FeCl_3$ and NaOH added to create an alkaline medium distilled water solution. Continuous stirring of Fe (II) Chloride and Fe (III) Chloride was formed Fe^{2+} and Fe^{3+} ions that further coprecipitate in alkaline medium and spherical Fe_3O_4 nano particles were obtained.

To prepare Ni nano particles, spherical metallic NiNPs were first synthesized, in the presence of sodium hydroxide, by the reduction of nickel (II) chloride with hydrazine hydroxide. The interaction between nickel(II) chloride and hydrazine solution produces a Ni complex. The addition of sodium hydroxide solution started series of reactions from the decomposition of the Ni complex via the formation of $Ni(OH)_2$ and eventually, the $Ni(OH)_2$ is reduced into spherical Ni nanoparticles [1].

Fe_3O_4 and Ni nanoparticles were coated with dopamine to help them stick to the polymer chains via the self-polymerization of dopamine [2].

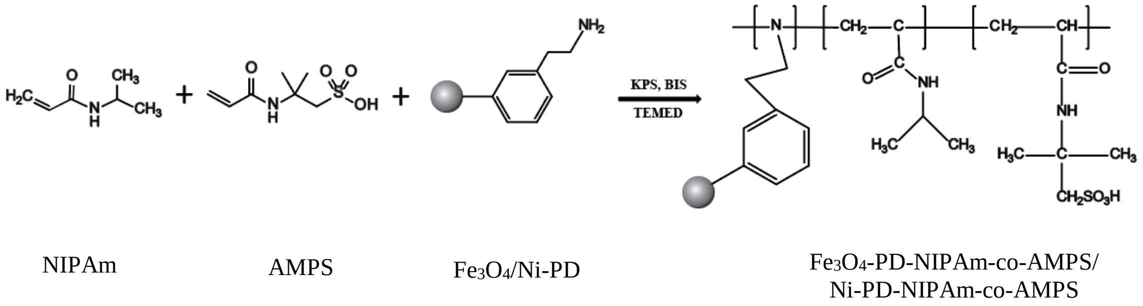

Figure 3.1.4 Schematic expression of synthesis of Fe_3O_4-PD-NIPAm-co-AMPS/ Ni-PD-NIPAm-co-AMPS hydrogels particles

Different types of copolymers where NIPAm as the main polymer chain and AMPS as a co-monomer were used. Copolymers are polymers that are made up of two or more monomer species. Here, anionic AMPS was used as a comonomer to remove different types of heavy metal ions because the anionic moiety shows selectivity towards a positive charge. AMPS contain a strongly ionizable sulfonate group that can easily remove metal ions from an aqueous solution. AMPS has high ionic moiety, and in the presence of ionic moiety, emulsion polymerization is very slow. To overcome the difficulties, TEMED was used as an accelerator during polymerization.

3.2 FTIR analysis of hydrogels

FTIR spectroscopy is widely used to characterize and quantify polymer blends, as well as to determine their compatibility through intermolecular hydrogen bonding and to explore their degradation processes. FTIR was used to characterize the composition and structure of Fe_3O_4, Fe_3O_4-PD, Fe_3O_4-PD-NIPAm-co-AMPS, Ni, Ni-PD and Ni-NIPAm-co-AMPS.

3.2.1 FTIR analysis of Fe_3O_4-PD-NIPAm-co-AMPS hydrogel

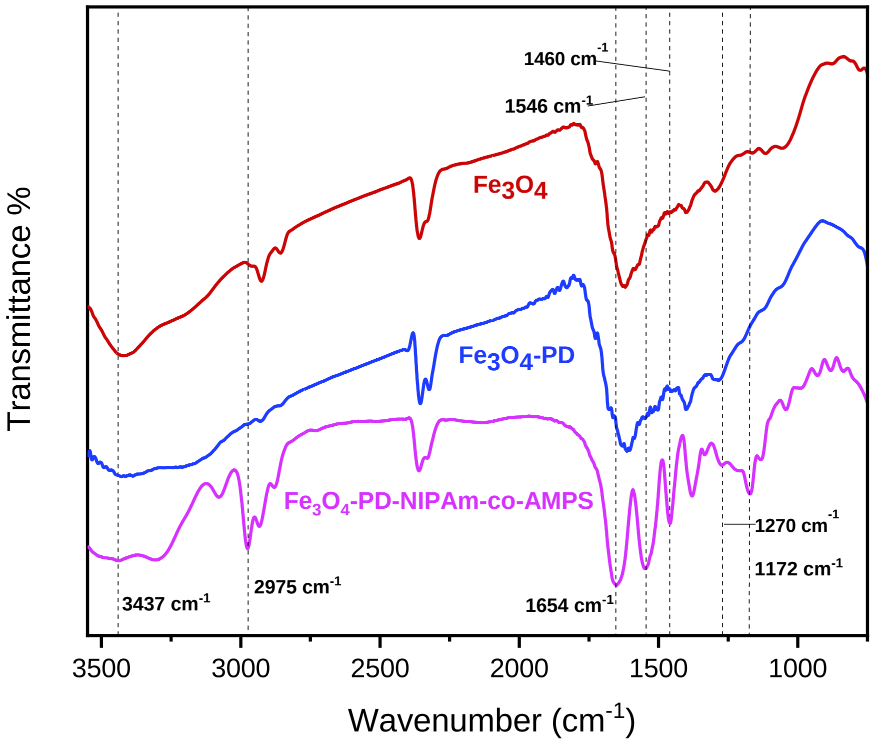

Figure 3.2.1 FTIR spectrum of Fe_3O_4, Fe_3O_4-PD, Fe_3O_4-PD-NIPAm-co-AMPS

In graph 3.2.1, red color line represents FTIR spectrum of Fe_3O_4, Blue color line represents FTIR spectrum of Fe_3O_4-PD, and violet color line represents FTIR spectrum of Fe_3O_4-PD-NIPAm-co-AMPS.

In the Fe_3O_4 FTIR line, two symbolic peaks around 1392 cm^{-1} and 585 cm^{-1} represent Fe-O stretching [3-5]. So, we can say that fabrication of our desired magnetic Fe_3O_4 is successful. The presence of polydopamine in the FTIR of Fe_3O_4-PD indicates by two characteristic bands; the band 1546 cm^{-1} was ascribed due to C=N and 3437 cm^{-1} ascribed to -OH stretching vibration. [6-8]. The magnetic phase bands of Fe-O around 1392 cm^{-1} and 585 cm^{-1} are also there. So, the fabrication of our desired Fe_3O_4-PD is successful.

In the FTIR spectrum of Fe_3O_4-PD-NIPAm-co-AMPS hydrogel particle, the peak around 2975 cm^{-1} indicates the -CH_2 stretching band [9-13]; the primary amide carbonyl group peaks of AMPS and NIPAm units and the secondary amide N-H deformation peaks are indicated by

1654 and 1546 cm^{-1} [14-18], respectively. The peak at 1460 cm^{-1} indicates C-H bending of CH_2 groups [19,20], at 1381 cm^{-1} indicates the vibration of the isopropyl group [19-22], at 1270 and 1172 cm^{-1} indicating the asymmetric and symmetric stretching of S = O bond of SO_3 groups. [23-25]. From physical appearance and FT-IR analysis, it may be concluded that the fabrication of our desired Fe_3O_4-PD-NIPAm-co-AMPS hydrogels particles is successful.

3.2.2 FTIR analysis of Ni-PD-NIPAm-co-AMPS hydrogel

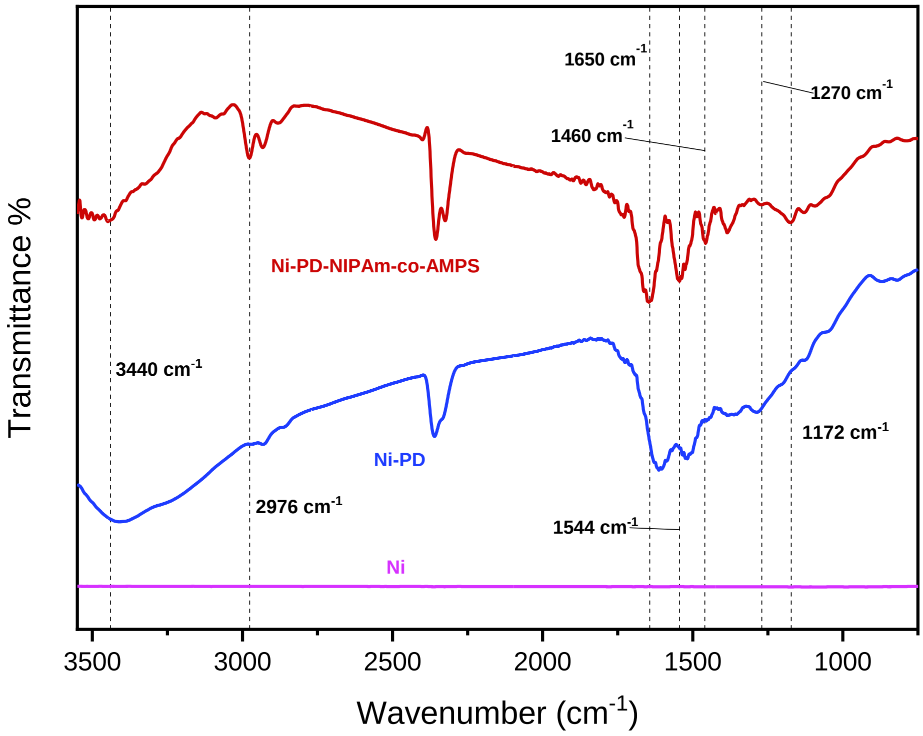

Figure 3.2.2 FTIR spectrum of Ni-PD-NIPAm-co-AMPS

FTIR was used to characterize the composition and structure of Ni, Ni-PD, Ni-PD-NIPAm-co-AMPS hydrogel particles. In graph 3.2.2, the violet color line represents FTIR spectrum of Ni, the blue color line represents FTIR spectrum of Ni-PD, and the red color line represents FTIR spectrum of Ni-PD-NIPAm-co-AMPS hydrogel particles.

The FTIR spectrum of Ni gives a straight line representing that the fabrication of our desired pure Ni nanoparticles is successful. The presence of Polydopamine in the FTIR of Ni-PD indicates by two characteristic bands; the band 1510 cm^{-1} was ascribed to C=N and 3440 cm^{-1}

ascribed to -OH stretching vibration. [4-6]. So, the fabrication of our desired Ni-PD is successful.

In FTIR spectrum of Ni-PD-NIPAm-co-AMPS hydrogel particles, the peak around 2975 cm^{-1} indicates the -CH_2 stretching band [9-13]; the primary amide carbonyl group peaks of AMPS and NIPAm units and the secondary amide N-H deformation peaks are indicated by 1654 and 1546 cm^{-1} [14-18], respectively. The peak at 1460 cm^{-1} indicates C-H bending of CH_2 groups [19,20], at 1381 cm^{-1} indicating the vibration of the isopropyl group [19-22], at 1270 and 1129 cm^{-1} indicating the asymmetric and symmetric stretching of S = O bond of SO_3 groups. [23-25]. From physical appearance and FT-IR analysis, it may be concluded that the fabrication of our desired Ni-PD-NIPAm-co-AMPS hydrogel particles is successful.

3.3 Scanning Electron Microscopy (SEM)

3.3.1 Scanning Electron Microscopy (SEM) analysis of Fe_3O_4 and Fe_3O_4-PD nanoparticles

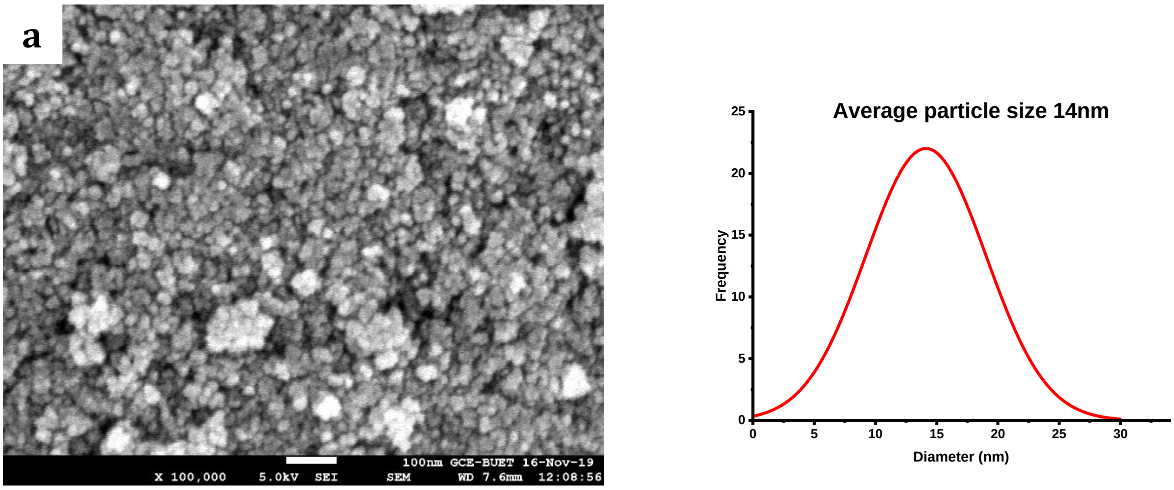

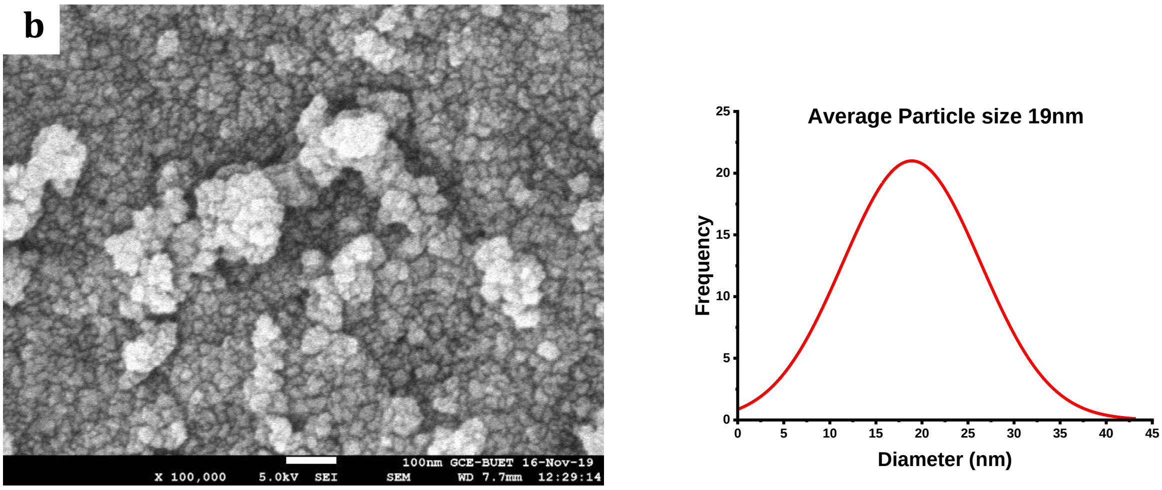

Figure 3.3.1 (a) SEM image of Fe_3O_4 (b) SEM image of Fe_3O_4-PD

The surface morphologies of the Fe_3O_4 and Fe_3O_4–PD nanoparticles were monitored by scanning electron micrographs. Figure 3.3.1(a) shows spherical and monodispersed Fe_3O_4 having an average diameter of ~14 nm, and Figure 3.3.1(b) shows Fe_3O_4 coated with polydopamine having an average size of ~19 nm. The creation of a 5 nm thick PD coating on the Fe_3O_4 nano particles was suggested by the increase in particle diameter (14 nm), which is consistent with prior results [26].

SEM analysis shows that the particle size of Fe_3O_4 is in nano range and particles are uniform. It was also found that after coating the Fe_3O_4 nano particles, the dopamine coated Fe_3O_4 nano particles size is still in the nano range and particles are uniform.

3.3.2 Scanning Electron Microscopy (SEM) analysis of Ni and Ni-PD nanoparticles

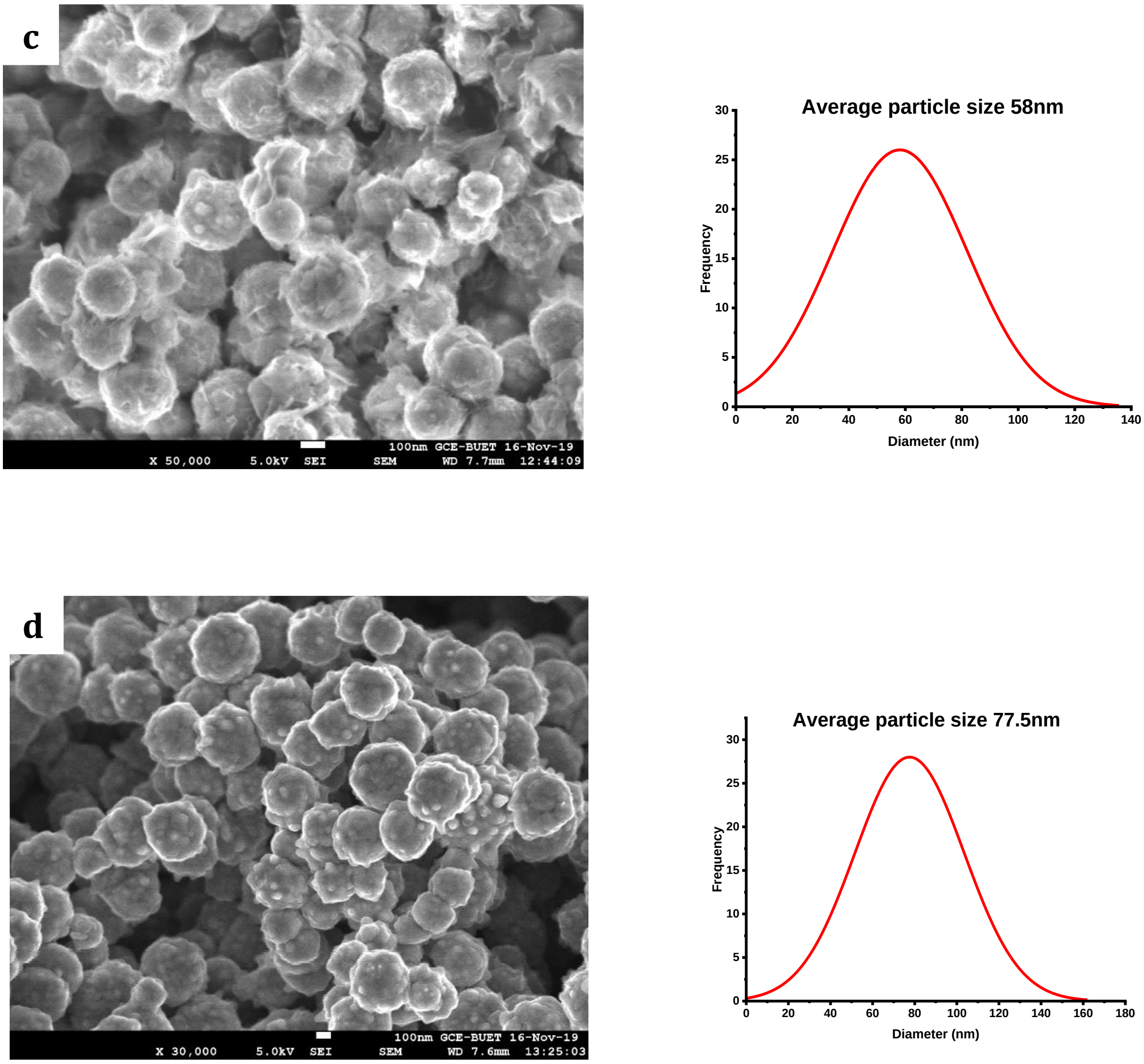

Figure 3.3.2 (a) SEM image of Ni (b) SEM image of Ni-PD

The surface morphologies of the Ni and Ni–PD nanoparticles were analyzed by scanning electron micrographs. Figure 3.3.2 (a) shows Ni nanoparticles having an average diameter of ~58 nm, and Figure 3.3.2 (b) shows Ni coated with polydopamine having an average size of ~77.5 nm. The creation of a 19.5 nm thick PD coating on the Fe_3O_4 nano particles was suggested by the increase in particle diameter (58 nm), which is consistent with prior results [27-28].

SEM analysis shows that the particle size of Ni is in nano range and particles are uniform. It was also found that after coating the Ni nano prticles, the dopamine coated Fe_3O_4 nano particles size is still in the nano range and particles are uniform.

3.4 Energy dispersive x-ray (EDX) spectral analysis

Element analysis of Fe_3O_4, PD-Fe_3O_4, and Ni and PD-Ni nanoparticles have been performed by Energy Dispersive X-ray (EDX) method.

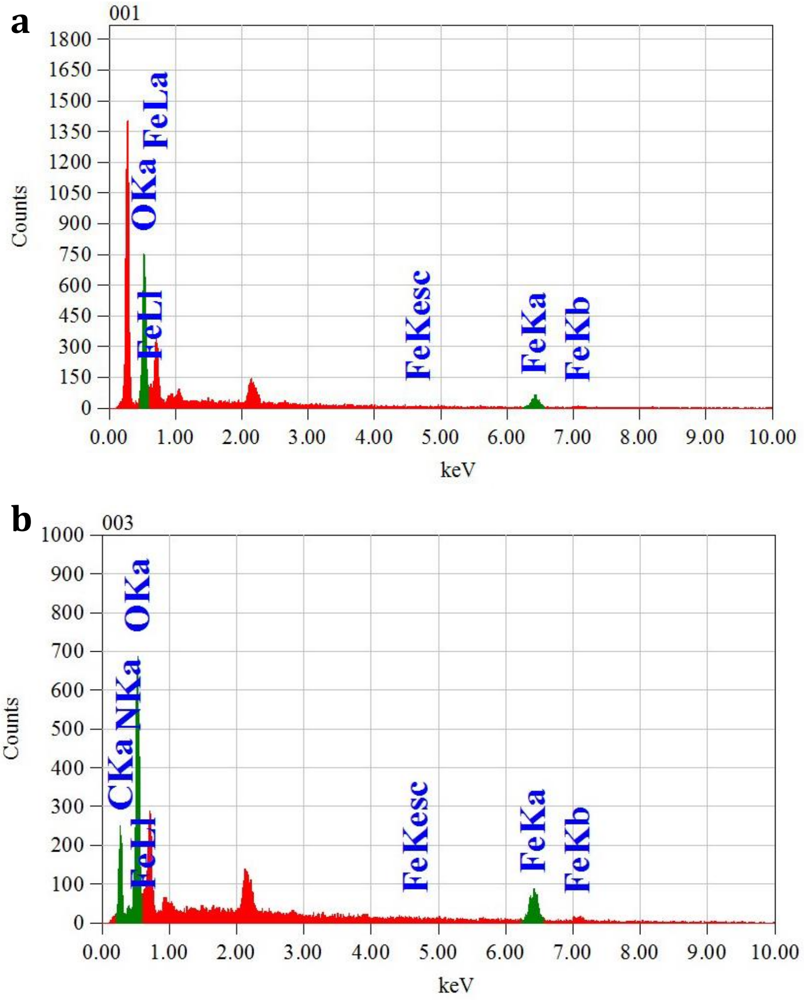

Element	**Atom%**
O	69.33
Fe	30.67

Element	**Atom%**
C	34.40
N	5.73
O	38.73
Fe	21.15

Figure 3.4.1(a) EDX analysis for Fe_3O_4 (b) EDX analysis for Fe_3O_4–PD

The EDX patterns are presented in Figure 3.4.1(a) shows peaks observed at 0.525, 6.398 keV for K lines of O, and Fe respectively. It indicates that the product is composed of Fe and O which is Fe_3O_4. In Figure 3.4.1(b) exhibits that the peaks appear at 0.277, 0.392, 0.525, 6.398 keV for K lines of C, N, O, and Fe, respectively. So EDX indicates that the surfaces of Fe_3O_4 nanoparticles are coated by polydopamine successfully. Two peaks appear around .9 amd 2.2 keV which are for Na and Cl. NaOH, $FeCl_2$ and $FeCl_3$ were used as reactants and a minor quantity of Cl and Na impurities were left behind with the Fe_3O_4 nano particles [29].

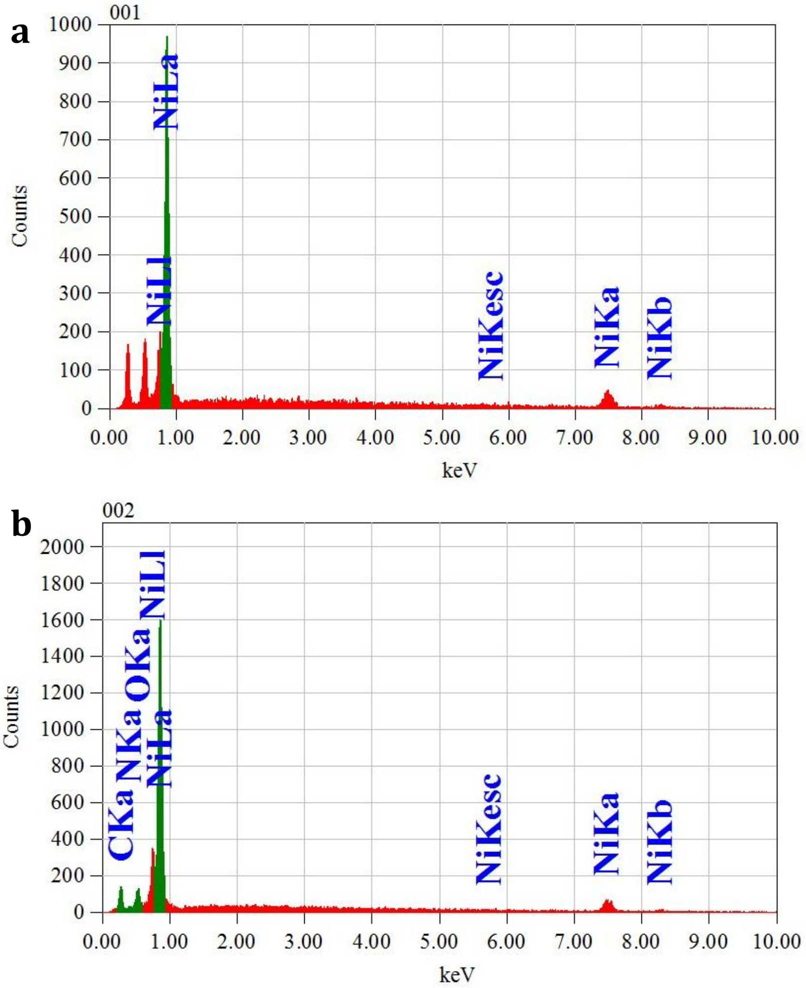

Element	**Atom%**
Ni	100

Element	**Atom%**
C	37.30
N	2.51
O	7.28
Ni	52.92

Figure 3.4.2(a) EDX analysis for Ni (b) EDX analysis for Ni–PD

Figure 3.4.2(a) exhibits that the peaks appear at 0.851 keV for L cell of Ni. Figure 3.4.2(b) shows that the peaks appear at 0.277, 0.392, 0.525 keV for K lines of C, N, O and 0.851 keV for L cell of Ni. So EDX indicates that the surfaces of Ni nanoparticles are successfully coated by polydopamine. Two peaks appear around .4 amd .6 keV which are for N and O. NaOH, N_2H_4 were used as reactants and a minor quantity of O and N impurities were left behind with the Ni nano particles.

3.5 Dynamic light scattering (DLS)

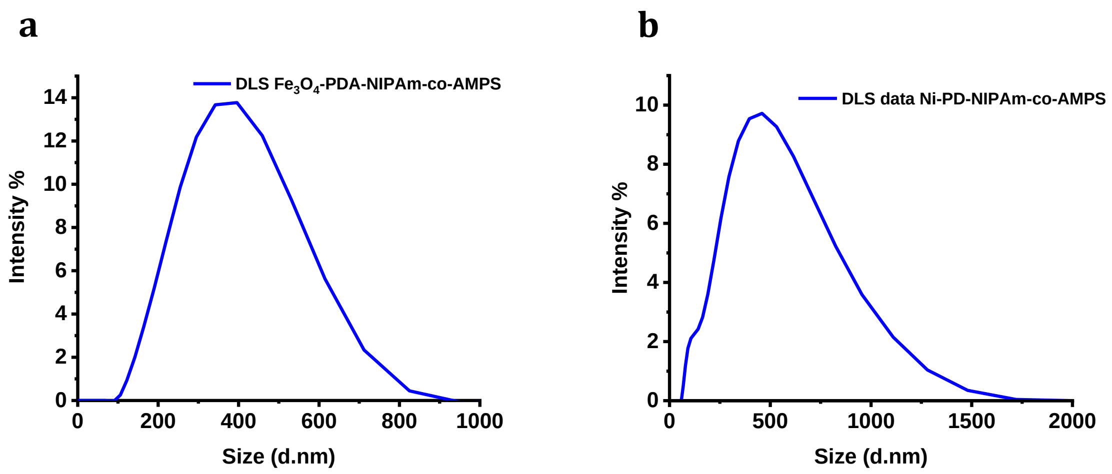

Figure 3.5.1(a) DLS analysis of Fe_3O_4-PD-NIPAM-co-AMPS submicrometer sized hydrogel, (b) DLS analysis of Ni-PD-NIPAM-co-AMPS submicrometer sized hydrogel.

DLS (dynamic light scattering) is a very powerful method for analyzing macromolecule diffusion in solution. DLS gives a measure of particle size-dependent time-related light scattering fluctuations (correlation function). This correlation function is first transformed into an intensity weighted diffusion coefficient, and subsequently into an intensity weighted hydrodynamic diameter, or Z-average value for dispersed particles [30-31].

The hydrodynamic size of Fe_3O_4-PD-NIPAM-co-AMPS and Ni-PD-NIPAM-co-AMPS gel particles were measured by DLS. Figure 3.5.1(a) shows that the average hydrodynamic size of Fe_3O_4-PD-NIPAM-co-AMPS nanogel particles is 403.9 nm. Figure 3.5.2(b) shows that the average hydrodynamic size of Ni-PD-NIPAM-co-AMPS particles is 305.4 nm.

3.6 Heavy metal removal analysis

3.6.1 Hg^{2+}removal analysis

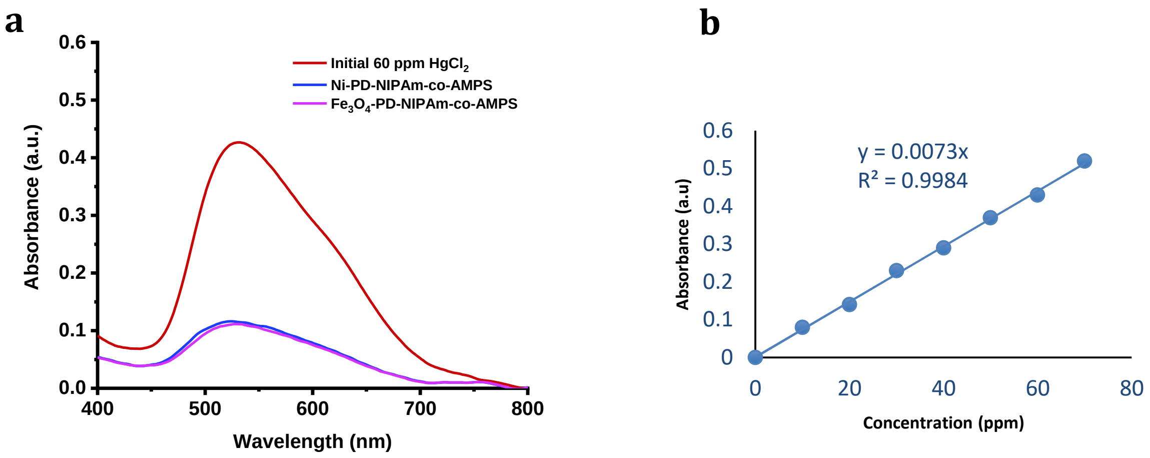

Figure 3.6.1 (a) Successive UV-Vis spectra of removing of Hg^{2+} by Fe_3O_4-PD-NIPAm-co-AMPS and Ni-PD-NIPAm-co-AMPS hydrogels particles(b) Calibration curve of Hg^{2+} concentration (ppm) vs absorbance (a.u.) value.

To calculate Hg^{2+} removal efficiency, UV-vis spectra was used. For quantitative analysis, a calibration curve of concentration (M) vs absorbance (a.u) of Hg^{2+} has been plotted and a linear line (y= mx) is observed. Using the calibration, the amount of Hg^{2+} removal efficiency has been measured. Different concentrations of Hg^{2+} solutions were used to create the calibration curve, and the change in absorbance was observed and reported using UV-vis spectra. The Hg^{2+} removal of efficiency of Fe_3O_4-PD-NIPAm-co-AMPS submicrometer-sized hydrogel is 167 mg/g. The Hg^{2+} removal of efficiency of Ni-PD-NIPAm-co-AMPS submicrometer-sized hydrogel is 162 mg/g.

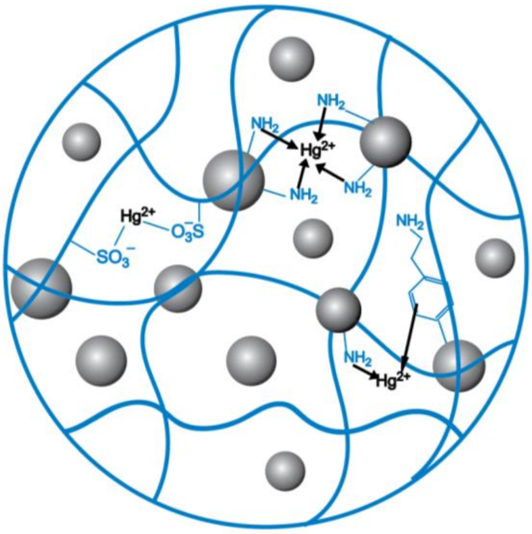

Image 3.6.2: Schematic expression of Hg^{2+}removal from water

Hg^{2+} was removed by the hydrogel network in different ways. There is ionic interaction between Hg^{2+} and SO^{3-} ion in the side chain of the polymer network. A coordination bond may form between NH_2 and Hg^{2+}. The benzene ring in the polymer chain may also form a bond with Hg^{2+}. Also, some Hg^{2+} may remove by the three-dimensional structure of hydrogel because of diffusion. The Hg^{2+} removal efficiency of Fe_3O_4-PD-NIPAm-co-AMPS and Ni-PD-NIPAm-co-AMPS hydrogels are, therefore, high.

3.6.2 Cr^{6+}removal analysis:

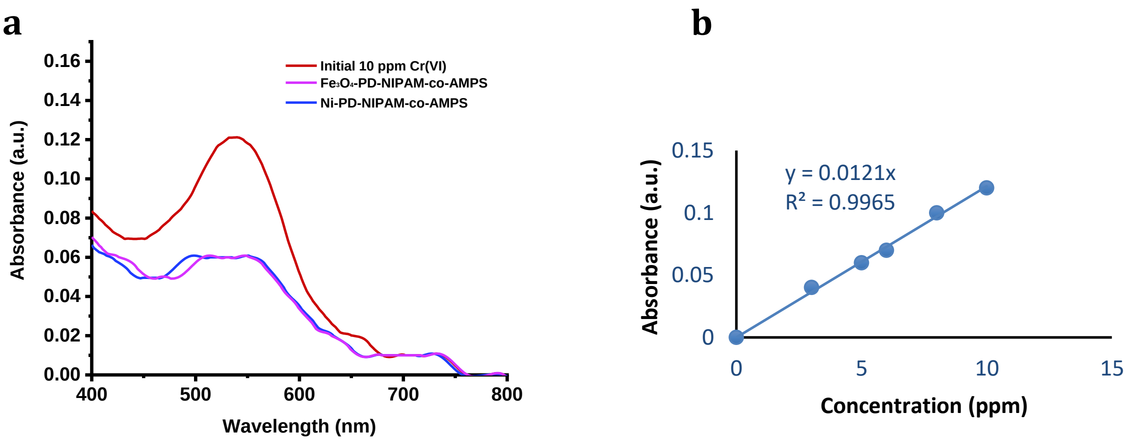

Figure 3.6.3 (a) Successive UV-vis spectra of removing of Cr^{6+} by Fe_3O_4-PD-NIPAm-co-AMPS and Ni-PD-NIPAm-co-AMPS submicrometer-sized hydrogel (b) Calibration curve of Cr^{6+} concentration (ppm) vs absorbance (a.u.) value.

To calculate Cr^{6+} removal efficiency UV-vis spectra was used. For quantitative analysis, a calibration curve of concentration (M) vs absorbance (a.u) has been plotted and a linear line (y= mx) is observed. Using the calibration, the amount of Cr^{6+} removal efficiency has been measured. Different concentrations of Cr^{6+} solutions were used to create the calibration curve, and the change in absorbance was observed and reported using UV-vis spectra. The Cr^{6+} removal of efficiency of Fe_3O_4-PD-NIPAm-co-AMPS nanogel is 8.837 mg/g. The Cr^{6+} removal of efficiency of Ni-PD-NIPAm-co-AMPS nanogel is 8.837 mg/g.

As Cr^{6+} stay in the water system as $Cr_2O_7^{2-}$, $HCrO^{4-}$ ions, there is no ionic interaction between the polymer chain and $Cr_2O_7^{2-}$. Some $Cr_2O_7^{2-}$ ions may remove from water because of diffusion. So, Cr^{6+} removal efficiency of Fe_3O_4-PD-NIPAm-co-AMPS and Ni-PD-NIPAm-co-AMPS is lower than Hg^{2+} removal efficiency. According to this study, Fe3O4-PD-NIPAm-co-AMPS and Ni-PD-NIPAm-co-AMPS are also effective in cationic solution, as are other hydrogels.

3.7 Magnetic Property of Hydrogel

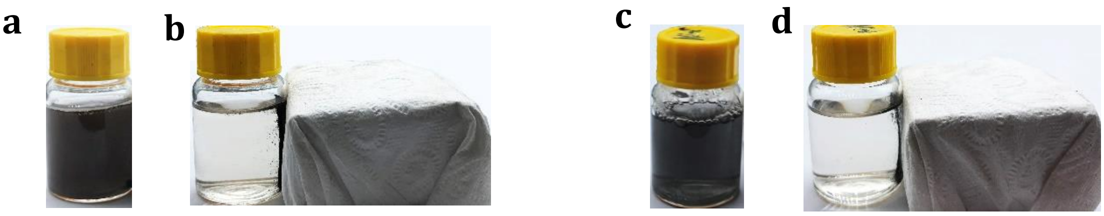

Figure 3.7 (a) Initial state of Fe_3O_4-PD-NIPAm-co-AMPS submicrometer-sized hydrogel particles (b) After 50 seconds of applying magnetic force (c) Initial state of Ni-PD-NIPAm-co-AMPS (d) After 50 seconds of applying magnetic force

After removing heavy metal ions submicrometer-sized hydrogels can separate from the medium easily by applying external magnetic force. Under the assistance of a Rare Earth Neodymium Magnet (70×30mm) N52 magnet, hydrogels were separated from the system. It took 90 seconds to separate most of the heavy metal-containing Fe3O4-PD-NIPAm-co-AMPS particles from water by applying external magnetic force and 50 seconds to remove most of the heavy metal Ni-PD-NIPAm-co-AMPS. So, initially, we can say that Ni-PD-NIPAm-co-AMPS submicrometer-sized hydrogel particles have stronger magnetic properties than Fe_3O_4-PD-NIPAm-co-AMPS submicrometer-sized hydrogel particles.

Reference:

[1] J. Y. Choi, Y. K. Lee, S. M. Yoon, H. C. Lee, B. K. Kim,J. M. Kim, K. M. Kim and J. H. Lee, A Chemical Route to Large-Scale Preparation of Spherical and Monodisperse Ni Powders”, *J. Am. Ceram. Soc.,* Vol. 88, pp. 3020–3023 (2005).

[2] J. Miao, H. Liu, W. Li and X. Zhang, “Mussel-Inspired Polydopamine-Functionalized Graphene as a Conductive Adhesion Promoter and Protective Layer for Silver Nanowire Transparent Electrodes”, *Langmuir*, Vol. 32, pp. 5365–5372 (2016).

[3] L. Yang *et al.*, “Modification and characterization of Fe3O4 nanoparticles for use in adsorption of alkaloids,” *Molecules*, Vol. 23, pp. 562 (2018).

[4] E. Bertolucci *et al.*, “Chemical and magnetic properties characterization of magnetic nanoparticles,” in *Conference Record - IEEE Instrumentation and Measurement Technology Conference*, 2015.

[5] D. Van Quy *et al.*, “Synthesis of silica-coated magnetic nanoparticles and application in the detection of pathogenic viruses,” *J. Nanomater.*, Vol. 2013, pp. 1-6 (2013).

[6] M. A. Pasquale, A. E. Bolzán, J. A. Güida, R. C. V. Piatti, A. J. Arvia, O. E. Piro, E. E. Castellano, "A new polymeric [Cu(SO3(CH2)3S–S(CH2)3SO3)(H2O)4]n complex molecule produced from constituents of a super-conformational copper plating bath: Crystal structure, infrared and Raman spectra and thermal behaviour," *Solid State Sciences*, Vol. 9(9), pp. 862–868 (2007).

[7] Y. Feng, A. Schmidt, R. A. Weiss, "Compatibilization of Polymer Blends by Complexation. 1. Spectroscopic Characterization of Ion−Amide Interactions in Ionomer/Polyamide Blends," *Macromolecules*, Vol. 29(11), pp. 3909–3917 (1996).

[8] S. H. Jou, M. Y. Shen, C. H. Yu, and Y. P. Lee, “Isomers of so3: Infrared absorption of OSOO in solid argon,” *J. Chem. Phys.*, Vol. 104(15), pp. 5745-5753 (1996).

[9] R. Manoharan, J. J. Baraga, R. P. Rava, R. R. Dasari, M. Fitzmaurice, and M. S. Feld, “Biochemical analysis and mapping of atherosclerotic human artery using FT-IR microspectroscopy,” *Atherosclerosis*, Vol. 103, pp. 181-193 (1993).

[10] J. Pironon and O. Barres, “Semi-quantitative FT-IR microanalysis limits: Evidence from synthetic hydrocarbon fluid inclusions in sylvite,” *Geochim. Cosmochim. Acta*, Vol. 54, pp. 509-518 (1990).

[11] F. Carrillo, X. Colom, J. J. Suñol, and J. Saurina, “Structural FTIR analysis and thermal characterisation of lyocell and viscose-type fibres,” *Eur. Polym. J.*, Vol. 40, pp. 2229-2234 (2004).

[12] J. Mihály, R. Deák, I. C. Szigyártó, A. Bóta, T. Beke-Somfai, and Z. Varga, "Characterization of extracellular vesicles by IR spectroscopy: Fast and simple classification based on amide and C[sbnd]H stretching vibrations," *Biochim. Biophys. Acta - Biomembr.*, Vol. 1859, pp. 459-466 (2017).

[13] D. L. Snavely and J. Dubsky, "Near-IR spectra of polyethylene, polyethylene glycol, and polyvinylethyl ether," *J. Polym. Sci. Part A Polym. Chem.*, Vol. 34(13), pp. 2575-2579 (1996).

[14] M. R. Oboodi, C. Alva, and M. Diem, "Solution-phase Raman studies of alanyl dipeptides and various isotopomers: A reevaluation of the amide III vibrational assignment," *Journal of Physical Chemistry*. Vol. 88(3), pp. 501–505 (1984).

[15] M. Diem, O. Lee, and G. M. Roberts, "Vibrational studies, normal-coordinate analysis, and infrared VCD of alanylalanine in the amide III spectral region," *J. Phys. Chem.*, Vol. 96(2), pp. 548–554 (1992).

[16] S. M. Lee, S. Y. Lin, and R. C. Liang, "Secondary conformational structure of type iv collagen in different conditions determined by fourier-transform infrared microscopic spectroscopy," *Artif. Cells, Blood Substitutes, Biotechnol.*, Vol. 23, pp. 193-205 (1995).

[17] G. M. Roberts, O. Lee, J. Calienni, and M. Diem, "Infrared Vibrational Circular Dichroism in the Amide III Spectral Region of Peptides," *J. Am. Chem. Soc.*, Vol. 110(6), pp. 1749–1752 (1988).

[18] M. Dunky, "Urea-formaldehyde (UF) adhesive resins for wood," *Int. J. Adhes. Adhes.*, Vol. 18, pp. 95-107 (1998).

[19] S. Senthilkumar, M. Briget Mary, and V. Ramakrishnan, "Infrared and Raman spectroscopic studies of L-valinium picrate," *J. Raman Spectrosc.*, Vol. 38, pp. 288-294 (2007).

[20] J. D. Debord, S. Eustis, S. Byul Debord, M. T. Lofye, and L. A. Lyon, "Color-tunable colloidal crystals from soft hydrogel nanoparticles," *Adv. Mater.*, Vol. 14(9), pp. 658-662 (2002).

[21] T. B. Freedman, X. Cao, R. V. Oliveira, Q. B. Cass, and L. A. Nafie, "Determination of the absolute configuration and solution conformation of gossypol by vibrational circular dichroism," *Chirality*, Vol. 15, pp. 196-200 (2003).

[22] Y. Katsumoto, A. Tsuchiizu, X. Qiu, and F. M. Winnik, "Dissecting the mechanism of the heat-induced phase separation and crystallization of poly(2-isopropyl-2-oxazoline) in water through vibrational spectroscopy and molecular orbital calculations," *Macromolecules*, Vol. 45(8), pp. 3531–3541 (2012).

[23] W. Cheng, F. Fan, Y. Zhang, Z. Pei, W. Wang, and Y. Pei, “A facile approach for fabrication of core-shell magnetic molecularly imprinted nanospheres towards hypericin,” *Polymers (Basel).*, Vol. 9(12), pp. 135 (2017).

[24] G. I. Dovbeshko, N. Y. Gridina, E. B. Kruglova, and O. P. Pashchuk, “FTIR spectroscopy studies of nucleic acid damage,” in *Talanta*, Vol. 53, pp. 233-246 (2000).

[25] Z. Ping, “In situ FTIR-attenuated total reflection spectroscopic investigations on the base-acid transitions of polyaniline. Base-acid transition in the emeraldine form of polyaniline,” *J. Chem. Soc. - Faraday Trans.*, Vol. 92, pp. 3063-3067 (1996)

[26] Y. P. He, S. Q. Wang, C. R. Li, Y. M. Miao, Z. Y. Wu, and B. S. Zou, “Synthesis and characterization of functionalized silica-coated Fe 3O4 superparamagnetic nanocrystals for biological applications,” *J. Phys. D. Appl. Phys.*, Vol. 38(9), pp. 1342-1350 (2005).

[27] T. Zeng, H.-y. Niu, Y.-r. Ma, W.-h. Li and Y.-q. Cai, “In situ growth of gold nanoparticles onto polydopamine-encapsulated magnetic microspheres for catalytic reduction of nitrobenzene” *Appl. Catal., B*, 2013, Vol. 134, pp. 26–33 (2013).

[28] J. Jiang, L. Zhu, L. Zhu, B. Zhu and Y. Xu, “Surface Characteristics of a Self-Polymerized Dopamine Coating Deposited on Hydrophobic Polymer Films” *Langmuir*, Vol. 27, pp. 14180–1418 (2011)

[29] L. Ai, C. Zeng, and Q. Wang, “One-step solvothermal synthesis of Ag-Fe3O4 composite as a magnetically recyclable catalyst for reduction of Rhodamine B”, *Catalysis Communications*, Vol. 141, pp. 68–73 (2011).

[30] A. L. Fernández, A. S. Castillo, L. Anderson, J. M. C. Fernández, S. D. Meister, R. Cecchini, L.F. C. Vallvey, M.C. M. Bondi, Marco, M. Pilar; J. C. S. López, I. S. Anderson, “A General Perspective of the Characterization and Quantification of Nanoparticles: Imaging, Spectroscopic, and Separation Techniques.” *Critical Reviews in Solid State and Materials Sciences*, Vol. 39, pp. 423–458 (2014).

[31] V. Uskoković, “Dynamic Light Scattering Based Microelectrophoresis: Main Prospects and Limitations”, *Journal of Dispersion Science and Technology*, Vol. 33(12), pp. 1762–1786 (2012).

CHAPTER 4
Conclusions

Conclusions

This work has given a new vision of research towards magnetic submicrometer-sized hydrogel. Different types of thermo and magnetic responsive nano hydrogels have been synthesized successfully where NIPAm is used as the main monomer and AMPS is used as comonomer where 70°C temperature is kept through the whole polymerization. Synthesized hydrogels particles are confirmed by FT-IR analysis. AMPS is used as a comonomer to insert the ionic component into the hydrogel. The size of submicrometer hydrogels is determined by DLS analysis and the average hydrodynamic size of Fe_3O_4-PD-NIPAM-co-AMPS and Ni-PD-NIPAM-co-AMPS hydrogel is 403.9 nm and 305.4 nm respectively. Preparing uniform size hydrogel particle is challenging, especially when an ionic monomer is used. To overcome those challenges SDS is used as a surfactant and TEMED is used as an accelerator. In this work, a facile route is developed to synthesize submicrometer-sized hydrogel particles.

Hydrogels are employed to remove Hg^{2+} and Cr^{6+} ions, with UV-vis spectroscopy revealing that both hydrogel particles have a high removal efficiency. It is difficult to extract hydrogel particles from wastewater after heavy metals are removed by them. To overcome those difficulties, the magnetic property is incorporated in the hydrogel. Fe_3O_4 and Ni are used to develop the magnetic property into submicrometer-sized hydrogel particles. Dopamine is coated on Fe_3O_4 and Ni nanoparticles to assist them to attach to polymer chains. At first, Fe_3O_4 and Ni nanoparticles are prepared and then coated the surface of nanoparticles by using dopamine. The average size and atom of nanoparticles and nanocomposites are observed by SEM and EDX analysis. Fe_3O_4-PD and Ni-PD nanoparticles have an average particle size in the nano range, according to SEM measurements.

Finally, as submicrometer-sized hydrogels particles are incorporated with magnetic properties, they can easily be separated from the medium after water treatment. A new door of research has been opened up to remove various heavy metals or hazardous chemicals from wastewater. Also, these hydrogel particles can be used in drug delivery, dye removal, drug delivery, contact lens, biosensor, tissue engineering, food industry, and so on. Further study is being carried out to investigate how these hydrogel particles behave in various environments, as well as how they change when different comonomers are incorporated.